



Paleo sea-level indicators and proxies from Greenland in the GAPSLIP database and comparison with modelled sea level from the PaleoMIST ice-sheet reconstruction

Evan J. Gowan^{1,2*}

¹Department of Earth and Environmental Sciences, Kumamoto University, Kumamoto, Japan; ²KIKAI Institute for Coral Reef Sciences, Kagoshima, Japan

Abstract

One of the most common ways to assess ice-sheet reconstructions of the past is to evaluate how they impact changes in sea level through glacial isostatic adjustment. PaleoMIST 1.0, a preliminary reconstruction of topography and ice sheets during the past 80 000 years, was created without a rigorous comparison with past sea-level indicators and proxies in Greenland. The basal shear stress values for the Greenland ice sheet were deduced from the present day ice-sheet configuration, which were used for the entire 80 000 years without modification. The margin chronology was based on previous reconstructions and interpolation between them. As a result, it was not known if the Greenland component was representative of its ice-sheet history. In this study, I compile sea-level proxy data into the Global Archive of Paleo Sea Level Indicators and Proxies (GAPSLIP) database and use them to evaluate the PaleoMIST 1.0 reconstruction. The Last Glacial Maximum (c. 20 000 years before present) contribution to sea level in PaleoMIST 1.0 is about 3.5 m, intermediate of other reconstructions of the Greenland ice sheet. The results of the data-model comparison show that PaleoMIST requires a larger pre-Holocene ice volume than it currently has to match the sea-level highstands observed around Greenland, especially in southern Greenland. Some of this mismatch is likely because of the crude 2500 year time step used in the margin reconstruction and the limited Last Glacial Maximum extent. Much of the mismatch can also be mitigated if different Earth model structures, particularly a thinner lithosphere, are assumed. Additional ice in Greenland would contribute to increasing the 3–5 m mismatch between the modelled far-field sea level at the Last Glacial Maximum and proxies in PaleoMIST 1.0.

1. Introduction

Sea-level change is one of the biggest threats to society, caused in part by the retreat of the Greenland ice sheet because of global warming (Fox-Kemper *et al.* 2021). Predicting future changes in sea level is essential to protect coastal infrastructure and human settlements. However, the magnitude and pattern of sea-level changes due to ice-sheet retreat is dependent on the past history of the ice sheet in a process known as glacial isostatic adjustment (GIA). GIA is the combined result of the balance between water stored in land-based ice and the ocean, time-variable Earth deformation caused by variations in the proportion of this storage, and changes to the Earth's gravity from changes in the distribution of mass. Since the Earth deformation is dependent on the history of ice- and water-loading, reconstructions of ice-sheet evolution in the past are needed to forecast the impact of changing sea levels. Greenland itself is strongly affected by GIA-induced changes in sea level that affect human settlements, and have been implicated, for instance, in the collapse of the Norse settlements in western Greenland (Borreggine *et al.* 2023).

The importance of the Greenland ice sheet for projecting future sea-level rise means that it has been the subject of many GIA-based reconstructions. Some such studies that focus on Greenland are highlighted here. Tarasov & Peltier (2002) tuned a dynamic ice-sheet model, based on a shallow ice

***Correspondence:** evangowan@gmail.com

Received: 14 Jun 2023

Revised: 30 Aug 2023

Accepted: 06 Sep 2023

Published: 13 Nov 2023

Keywords: glacial isostatic adjustment, ice sheets, sea level, Holocene, model-data comparison

Abbreviations:

GAPSLIP: Global Archive of Paleo Sea Level Indicators and Proxies

GIA: glacial isostatic adjustment

GRIP: Greenland Ice Core Project

GSHHG: Global Self-consistent,

Hierarchical, High-resolution Geography Database

HOLSEA: Holocene relative sea level

kyr BP: thousand years before present

LGM: Last Glacial Maximum

PaleoMIST: Paleo ice sheet margins, ice sheets and topography

PALSEA: Paleo constraints on sea level rise

SLE: sea level equivalent

GEUS Bulletin (eISSN: 2597-2154) is an open access, peer-reviewed journal published by the Geological Survey of Denmark and Greenland (GEUS). This article is distributed under a [CC-BY 4.0](https://creativecommons.org/licenses/by/4.0/) license, permitting free redistribution and reproduction for any purpose, even commercial, provided proper citation of the original work. Author(s) retain copyright.

Edited by: Signe H Larsen (GEUS, Denmark)

Reviewed by: William Colgan (GEUS, Denmark); Sarah Bradley (The University of Sheffield, UK)

Funding: See page 13

Competing interests: See page 13

Additional files: 13

approximation, using Holocene relative sea-level observations and temperature and age profiles from the Greenland ice core project (GRIP) ice core. This reconstruction is also used in the global ICE-5G (Peltier 2004) and ICE-6G (Peltier *et al.* 2015) reconstructions. Fleming & Lambeck (2004) investigated the Greenland ice sheet using flowline-based reconstructions originally created by Hughes (1981) and Hughes *et al.* (1981), and scaled versions of them. Simpson *et al.* (2009) and Lecavalier *et al.* (2014) created a reconstruction using a dynamic ice-sheet model, based on a shallow ice approximation, tuned to fit sea-level changes and ice extent at the Last Glacial Maximum (LGM).

PaleoMIST 1.0 (Paleo ice-sheet Margins, Ice Sheets and Topography) is a global ice sheet and topography reconstruction for the past 80 000 years at 2500 year time intervals (Gowan *et al.* 2021). The ice-sheet component was created using the perfectly plastic ice-sheet model ICESHEET (Gowan *et al.* 2016a) using ice-sheet margins that were constrained from chronological, geological, and geomorphological constraints. The ice-sheet reconstruction was refined through a number of iterations using the GIA model SELEN (Spada & Stocchi 2007; de Boer *et al.* 2014, 2017). This reconstruction is considered to be preliminary, because of its coarse time step (2500 years), and the fact that it was only evaluated

against sea-level indicators and proxies in the centre of the Laurentide and Eurasian ice sheets. These ice masses were the largest contributors to sea-level variations during the past 80 000 years, therefore smaller contributors such as the Greenland ice sheet were not rigorously evaluated.

In this paper, I compare deglacial period sea-level indicators and proxies from Greenland with the sea-level response calculated from PaleoMIST 1.0. To accomplish this, I compiled the indicators and proxies into an online database called GAPSLIP (Global Archive of Paleo Sea Level Indicators and Proxies). My goal is to demonstrate the misfit of the current reconstruction to sea-level indicators and proxies to guide future refinements. Further refinements on the geologically constrained ice-sheet margin and directions of ice flow will be needed to make a more robust reconstruction. It is also necessary to take into account multiple possibilities for the Earth rheology structure.

2. Sea-level data indicators and proxies

2.1 Archives of sea-level data

Since 2008, the PALSEA (PALEO constraints on SEA level rise) project has strived to gather scientists interested

Table 1 Sea-level proxies and indicators across Greenland

Location	<i>n</i>	Marine limiting	Terrestrial limiting	Index points	References
North-eastern Greenland					
Kap Morris Jesup	73	67	6	0	Ives <i>et al.</i> (1964); Funder (1982); Möller <i>et al.</i> (2010); Funder <i>et al.</i> (2011a)
Danmark Fjord	30	27	0	3	Tauber (1960, 1961, 1964); Trautman (1963); Ives <i>et al.</i> (1964); Funder (1982); Håkansson (1982); Hjort (1997); Funder <i>et al.</i> (2011a); Bennike & Weidick (2001)
Frederick E. Hyde Fjord	16	14	1	1	Weidick (1972a, 1973, 1977); Funder (1982); Landvik <i>et al.</i> (2001)
Germania Land	14	14	0	0	Landvik (1994)
Hochstetter Forland	20	12	8	0	Weidick (1977); Håkansson (1978, 1981); Hjort (1979, 1981); Björck <i>et al.</i> (1994b)
Hold With Hope	17	16	0	1	Hjort & Funder (1974); Håkansson (1975); Weidick (1976, 1977); Hjort (1979)
Independence Fjord	12	11	1	0	Rubin & Alexander (1960); Ives <i>et al.</i> (1964); Tauber (1966); Weidick (1977); Funder (1982); Funder & Abrahamsen (1988); Bennike (2002); Funder <i>et al.</i> (2011a);
J.P. Koch Fjord	2	2	0	0	Landvik <i>et al.</i> (2001)
Jameson Land	17	12	5	0	Funder (1971, 1972, 1973, 1978, 1990a); Weidick (1972a, 1973, 1974); Hjort (1979); Ingólfsson <i>et al.</i> (1994); Björck <i>et al.</i> (1994a); Funder & Hansen (1996)
Kap Clarence Wyckoff	32	29	0	3	Ives <i>et al.</i> (1964); Tauber (1964); Funder (1982); Funder & Abrahamsen (1988); Funder <i>et al.</i> (2011a)
Kempe Fjord	10	10	0	0	Håkansson (1973, 1974, 1976); Hjort & Funder (1974); Weidick (1977); Hjort (1979)
Kong Oscar Fjord	53	50	0	3	Washburn & Stuiver (1962); Trautman (1963); Lasca (1966); Håkansson (1972, 1973, 1974, 1975, 1976); Hjort & Funder (1974); Hjort (1979)
Nansen Land	6	6	0	0	Weidick (1973); Kelly & Bennike (1985, 1992); Bennike & Kelly (1987); Landvik <i>et al.</i> (2001)
Nioghalvfjærdsfjorden	17	17	0	0	Bennike & Weidick (2001)
Prinsesse Ingeborg Halvø	67	63	1	3	Ives <i>et al.</i> (1964); Funder (1982); Håkansson (1987); Funder & Abrahamsen (1988); Bennike (1997); Hjort (1997); Funder <i>et al.</i> (2011a); Strunk <i>et al.</i> (2018) Tauber (1961)
Renland	5	4	1	0	Funder (1971); Hjort & Funder (1974)
Schuchert Dal	97	63	0	34	Funder (1972, 1978); Weidick (1972a); Street (1977); Hjort (1979); Funder & Hansen (1996); Hall <i>et al.</i> (2008, 2010)
Trail Ø	19	18	0	1	Håkansson (1972, 1973, 1974); Hjort (1973, 1979); Hjort & Funder (1974)
Young Sund	27	8	6	13	Weidick (1977); Hjort (1979); Christiansen <i>et al.</i> (2002); Pedersen <i>et al.</i> (2011); Bennike & Wagner (2012)

Table 1 (continued) Sea-level proxies and indicators across Greenland

Location	<i>n</i>	Marine limiting	Terrestrial limiting	Index points	References
North-western Greenland					
Bessel Fjord	36	3	0	33	Weidick (1977); Blake (1987a); Bennike (2002); McNeely & Brennan (2005); Glueder <i>et al.</i> (2022)
Kangerluarsuk (Cass Fjord)	16	15	1	0	Weidick (1977); Blake (1987a); Bennike (2002); McNeely & Brennan (2005)
Hall Land	66	37	0	29	Rubin & Alexander (1960); England (1985); Kelly & Bennike (1985, 1992); Bennike & Kelly (1987); McNeely & McCuaig (1991); McNeely & Brennan (2005); Glueder <i>et al.</i> (2022)
Inglefield Fjord	10	6	4	0	Weidick (1976); Fredskild (1985); Blake <i>et al.</i> (1996)
Nordvestø	3	3	0	0	Kelly <i>et al.</i> (1999)
Thule	11	10	0	1	Funder (1990b); Kelly <i>et al.</i> (1999)
Tuttulissuaq	1	0	1	0	Blake (1987b); Fredskild (1985)
Warming Land	4	4	0	0	Kelly & Bennike (1985, 1992); Bennike & Kelly (1987)
Wulff land	3	3	0	0	Bennike & Kelly (1987); Kelly & Bennike (1992)
South-eastern Greenland					
Ammassalik	6	0	2	4	Long <i>et al.</i> (2008, 2011)
South-western Greenland					
Akullit	24	10	1	13	Weidick (1972a, 1974, 1976); Jungner (1979); Long & Roberts (2002); Long <i>et al.</i> (2011)
Alluttoq Island	10	0	2	8	Long <i>et al.</i> (1999, 2006, 2011)
Eqalussuit Tasiat	5	5	0	0	Weidick (1972a, 1974)
Ikertoq Fjord	7	5	0	2	Weidick (1972a, 1973); Ten Brink & Weidick (1974); Ten Brink (1975); van Tatenhove <i>et al.</i> (1996)
Ilulissat	12	2	3	7	Weidick (1972a, 1973); Long <i>et al.</i> (2006, 2011)
Itilleq	11	2	0	9	Weidick (1972a); Long <i>et al.</i> (2009, 2011)
Kangerluk	9	0	0	9	Föged (1989); Bennike (1995); Rasch (1997); Long <i>et al.</i> (2011); Souza <i>et al.</i> (2021)
Kangerlussuaq	34	20	4	10	Weidick (1972a, 1972b, 1973); Ten Brink & Weidick (1974); Ten Brink (1975); van Tatenhove <i>et al.</i> (1996); Storms <i>et al.</i> (2012); Bierman <i>et al.</i> (2018)
Kannala	33	3	3	27	Weidick (1974, 1976); Jungner (1979); Long <i>et al.</i> (2003, 2011); Long & Roberts (2003)
Kapisillit	26	8	17	1	Weidick (1968, 1972b, 1975, 1976); Fredskild (1973, 1983); McGovern <i>et al.</i> (1996); Weidick <i>et al.</i> (2012); Larsen <i>et al.</i> (2014)
Maniitsoq	5	5	0	0	Weidick (1973)
Nanortalik	24	0	0	24	Bennike <i>et al.</i> (2002); Sparrenbom <i>et al.</i> (2006b); Long <i>et al.</i> (2011)
Nuuk	44	25	19	0	Weidick (1973, 1976); Fredskild (1983); Berglund (2003); Hinnerson-Berglund (2004); Larsen <i>et al.</i> (2014, 2017)
Paamiut	10	0	1	9	Woodroffe <i>et al.</i> (2014)
Qaqortoq	30	11	0	19	Weidick (1975); Bennike <i>et al.</i> (2002); Sparrenbom <i>et al.</i> (2006a); Fredh (2008); Randsalu (2008); Long <i>et al.</i> (2011); Bierman <i>et al.</i> (2018)
Qeqertarsuatsiaat	11	11	0	0	Weidick (1975); Larsen <i>et al.</i> (2014)
Sisimiut	12	3	0	9	Weidick (1972a, 1973); Bennike <i>et al.</i> (2011); Long <i>et al.</i> (2011)
Tasiussarsuaq	13	4	9	0	Lasher <i>et al.</i> (2020)

in past sea-level variability to deduce changes in ice sheet and ocean volume (Carlson *et al.* 2019). For the period after the LGM, there has been an effort by PALSEA to compile sea-level indicators and proxies in a standardised way through the associated HOLSEA (HOLocene relative SEA level) project (Khan *et al.* 2019). A standardised database for all of Greenland has yet to be published. The only data set currently available for Greenland that is considered to be compatible with the HOLSEA standards is that for isolation basins (Long *et al.* 2011).

For the purposes of assessing reconstructions of the Greenland ice sheet, a broader database is required. For this study, I have compiled data for all of Greenland (Table 1, Fig. 1). This compilation is not done with the same level of rigour as a HOLSEA-style database, but rather is an interim product that will be replaced when such a study becomes available.

These data are part of the broader GAPSLIP database. The database format contains fewer fields than the HOLSEA data sets, as it is intended to be used in conjunction with comparisons with modelled sea level from GIA. The initial construction of this database structure began during previous GIA assessment studies (Gowan *et al.* 2016b, 2021). The current version of GAPSLIP (2.0) features a completely revamped code structure and many bug fixes, and data derived from over 1000 studies. In addition to the Greenland data set described in this paper, it also incorporates HOLSEA and HOLSEA-compatible databases for eastern Canada (Vacchi *et al.* 2018), eastern United States (Engelhart & Horton 2012), the Baltic Sea (Rosentau *et al.* 2021), North Sea (Vink *et al.* 2007), northern Russia (Baranskaya *et al.* 2018), Southeast Asia (Mann *et al.* 2019), Australia (Larcombe *et al.* 1995; Belperio *et al.* 2002; Sloss *et al.* 2007;

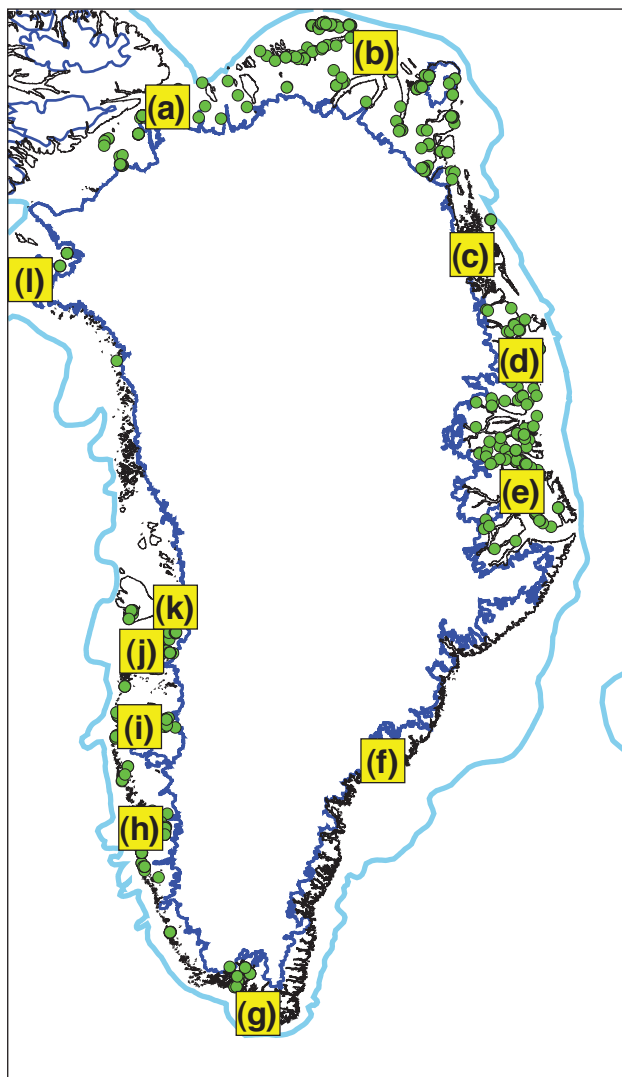


Fig. 1 Map showing the locations of the 47 subregions for which there are data in the GAPSLIP database for Greenland and the present-day and LGM grounded ice-sheet margin from PaleoMIST. The locations with data-model comparisons shown in Fig. 5 are labelled as follows: (a) Hall Land (b) Kap Clarence Wyckoff (c) Germania Land (d) Young Sund (e) Schuchert Dal (f) Ammassalik (g) Nanortalik (h) Nuuk (i) Ikertooq Fjord (j) Kannala (k) Alluttoq Island (l) Thule.

Lewis *et al.* 2013), and Antarctica (Briggs & Tarasov 2013; Ishiwa *et al.* 2021). Data from the LGM and Marine Isotope Stages 3 and 4 (70 000–27 000 yr BP) are also included (Gowan *et al.* 2022). The database can be found on Github (https://github.com/evangowan/paleo_sea_level) and will be periodically updated. All radiocarbon dates have been recalibrated using OxCal (Bronk Ramsey 2009) using the latest calibration curves (Heaton *et al.* 2020; Hogg *et al.* 2020; Reimer *et al.* 2020). The ages in this paper are reported as kyr BP (thousands of years before present, where present is defined as the year 1950).

2.2 Data compilation

Although a data compilation has not been published for Greenland, a comprehensive list of studies that have sea-level data is contained in Lecavalier *et al.* (2014). All of the references listed in that paper were checked and the relevant data were included. Radiocarbon date lists from laboratories that frequently published data from Greenland were also checked. I conducted a literature search to find papers published after Lecavalier *et al.* (2014). In total, there are 1019 data points, which were split into 47 subregions to minimise a possible gradient in the GIA signal and to ensure that data cluster geographically (Table 1). The names of the subregions were taken from a geographical feature within that area. The data include marine-limiting points (where sea level was located above the elevation of the sample), terrestrial-limiting points (where sea level was located below the elevation of the sample), and sea-level indicators (also called index points) that provide an estimate of past sea-level position within a certain elevation range. Note that this compilation does not take into account the possibility of tectonically-induced elevation changes, such as the suspected magnitude >8 earthquake that happened in the Early Holocene in southern Greenland (Steffen *et al.* 2020). Data-model comparison plots for all 47 subregions can be found in the Supplementary File S1. An example of the data from Kangerlussuaq as plotted in the GAPSLIP database is given in Fig. 2.

In some cases, the locations of the data were not explicitly stated, and it had to be estimated based on maps and descriptions in the original studies. I used Google Earth™ to estimate the location in these cases. The location provided by Google Earth may have uncertainties in the order of 10s of km in places, since the satellite imagery was rectified using GSHHG (Global Self-consistent, Hierarchical, High-resolution Geography Database; Wessel & Smith 1996), which is inaccurate in Greenland [For details on the inaccuracy, see *here*: <https://github.com/GenericMappingTools/gshhg-gmt/issues/12>, see also Henriksen *et al.* (2000)]. This issue may introduce errors in the model-data comparison, depending on the gradient of the GIA response. The plots in this paper use a coastline extracted from the BEDMACHINE Greenland version 5 topography dataset (Morlighem *et al.* 2017, 2022) to avoid this problem.

2.3 Vertical interpretation and elevation uncertainties

To be a useful constraint, sea-level indicators and proxies must provide context on the past sea-level position relative to present day. Geomorphic-based indicators provide an 'indicative meaning', in which the relative position of past sea level can be determined based on

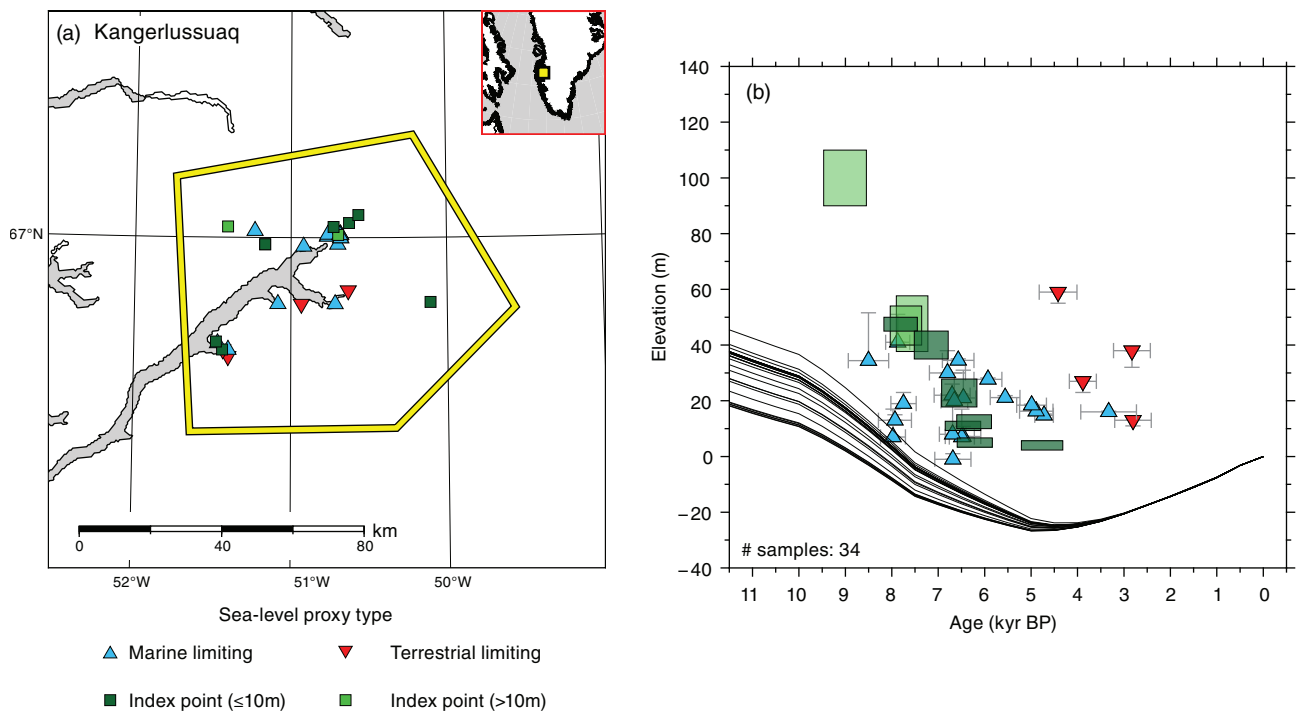


Fig. 2 Paleo sea level and comparison with the reference model at Kangerlussuaq subregion. (a) A map of the locations of the data, including a **yellow outline** that defines the subregion. This location demonstrates the four classes of data, including **marine limiting** (sea level was above the data point), **terrestrial limiting** (sea level was above the data point), and **index points** (sea level was within a bounded elevation range), which has different shades depending on whether or not the uncertainty is less or greater than 10 m. (b) The elevation of the proxy data with uncertainty ranges, and the calculated sea level at the location of each point from the reference PaleoMIST 1.0 model. There is a gradient in the calculated sea level in this area, so multiple calculated sea-level curves are visible. Data uncertainties are displayed at 2σ . Data references: Weidick (1972a, b, 1973); Ten Brink & Weidick (1974); Ten Brink (1975); van Tatenhove *et al.* (1996); Storms *et al.* (2012); Bierman *et al.* (2018).

a modern analogue and within a range of uncertainty (Rovere *et al.* 2016). For instance, a beach deposit will form between the ordinary berm (the upper limit of wave-generated deposition) and the breaking depth of waves. Another indicator is an isolation basin, where the transition of the basin from marine to lacustrine deposits will provide the timing for when sea level was positioned at the outlet of a basin (Long *et al.* 2011). In cases where samples are in littoral deposits, they can only be judged as marine limiting and that sea level was above the elevation of the deposits. Likewise, archaeological and terrestrial deposits can only indicate that sea level was below the elevation of the sample. Most of the data from Greenland are terrestrial or marine limiting (Table 1). Redeposited shells in diamicton and glacial till generally cannot be used as proxies because the geological context cannot be determined.

Many of the data in the database are from marine shells, with a limited description of the geological context of the deposits. For these data, it is not possible to interpret the water depth, therefore they are included as marine-limiting indicators. Where the shells are reported from beach or beach ridge deposits, it is possible to infer a sea-level index point. In these cases, the programme IMCalc was used to produce the uncertainty range (Lorscheid & Rovere 2019). This programme uses models of tidal range and wave heights

to infer the uncertainty of the indicative meaning of the deposits.

One of the largest sources of data in the database comes from an archive of driftwood from northern and north-eastern Greenland reported by Funder *et al.* (2011a). The driftwood was reported as generally deposited 1–2 m above sea level by storm action, but the authors warned that some samples had likely moved downslope after deposition. The driftwood gives maximum ages for the sea-level position as the trees grew for an unknown time before deposition, and the area where the driftwood was found was undergoing post-glacial uplift, I have therefore, conservatively, included these data as marine limiting, after subtracting 2 m from the reported elevation.

To compare sea-level indicator and proxy data to modelled sea level, it is necessary to ensure the elevation of the data is reported relative to a known datum, usually mean sea level. The uncertainty on the elevation measurements depend on the technique used. For instance, elevation measurements from differential GPS can achieve a precision of less than 10 cm, while elevations derived from topographic maps can be in the order of metres (Rovere *et al.* 2016). In studies where the method used to determine elevation is clearly described, I have used the reported elevation uncertainty. However, the vast majority of the studies incorporated into the

database do not report uncertainties, the datum used for the elevation, the tidal range or details on how the elevation was measured. In these cases, I have applied an uncertainty based on the recommendations in Rovere *et al.* (2016). For reported elevations less than 5 m, an uncertainty of ± 1 m is applied. For reported elevations above 5 m, $\pm 20\%$ of the reported elevation is applied, up to a maximum of ± 10 m. This level of uncertainty is justified, as it has been reported that some of the reported elevations of legacy Greenland data have errors in the order of 10 m (Woodroffe *et al.* 2014).

2.4 Age control

The vast majority of the age constraints of the sea-level indicators and proxies come from radiocarbon dates (990 points), though there are also some constraints from optically stimulated luminescence (11 points), cosmogenic ^{10}Be (15 points), and age models (2 points). All of the data, including calibrated radiocarbon dates, are displayed at 2σ limits.

Conventional radiocarbon dates are corrected for the isotopic fractionation of carbon by normalising to $\delta^{13}\text{C} = -25\text{‰}$ relative to the PeeDee Belemnite standard (Stuiver & Polach 1977). Many early radiocarbon laboratories did not follow this standard, and therefore those dates need to be corrected for the fractionation effect before calibration. A large portion of the dates in this database come from marine carbonates that have a value of approximately $\delta^{13}\text{C} = 0\text{‰}$, which equates to a roughly 400 year offset if not corrected. Some laboratories did correct for fractionation, but unconventionally normalised marine carbonates to this value. All the laboratory procedures are documented at https://github.com/evangowan/radiocarbon_labs. Where a fractionation correction was required, I used the estimated values of $\delta^{13}\text{C}$ listed in Stuiver & Polach (1977).

Marine carbonate radiocarbon ages need correction for the offset in age from the atmosphere because of the marine carbon reservoir. The reservoir corrections are derived from the Calib reservoir age database (Reimer & Reimer 2001). For the purposes of correcting data from Greenland, I have used two corrections, one for the part of Greenland adjacent to Baffin Bay, and another for the rest of Greenland (Table 2).

3. Model-data comparison

3.1 The PaleoMIST reconstruction of Greenland

PaleoMIST 1.0 is a preliminary ice-sheet and topography reconstruction for the past 80 000 years at 2500 year resolution (Gowan *et al.* 2021). The goal of this reconstruction was to create a generalised depiction of ice-sheet evolution over this period based on geological and geophysical evidence from the core areas of the North American and Eurasian ice sheets, which contributed to the majority of sea-level changes during the last glacial cycle. The ice sheets were constructed using the plastic ice-sheet model ICESHEET (Gowan *et al.* 2016a) assuming equilibrium conditions. In the most basic version of this model (i.e. without variations in base topography or shear stress), the change in ice-surface elevation, E , at a distance, s , along a flowline is related to the basal shear stress τ_0 through the following equation (Cuffey & Paterson 2010):

$$\frac{dE}{ds} = \frac{\tau_0}{\rho_i g H}$$

The density of ice is ρ_i and g is the gravity at the surface of the Earth. In this formulation, the ice-sheet surface profile is approximated as a parabolic shape. The primary variables in the model were the ice margin and basal shear stress, which control the steepness of the ice-surface profile. The ice margins were largely based on previously published margin reconstructions or geological evidence (e.g. Dyke 2004; RAISED Consortium *et al.* 2014; Hughes *et al.* 2016; Dalton *et al.* 2019). The initial basal shear stress values for the paleo ice sheets in Europe and North America were parameterised based on topographic and surficial geological considerations. These values were further adjusted to improve the misfit between the modelled sea level and geological evidence of sea-level change in the core regions of the North American and Eurasian ice sheets (Baranskaya *et al.* 2018; Vacchi *et al.* 2018; Rosentau *et al.* 2021). In general, it was set so the shear stress values decrease during deglaciation, as the ice sheets likely thinned before the margin retreated. The base topography used for the reconstruction was RTopo-2 (Schaffer

Table 2 Reservoir age used to correct marine carbonates

Location	Reservoir age	Calib Map Number ¹	References
Western Greenland including Baffin Bay, Davis Strait and Nares Strait	39 ± 107	9, 10, 11, 34, 35, 36, 37, 38, 39, 40, 665, 666, 721, 724, 725, 726, 727, 728, 729, 730, 782, 786, 787, 788, 789, 986, 987, 988, 989, 990, 2062	Olsson (1980); Mörner & Funder (1990); McNeely <i>et al.</i> (2006); Coulthard <i>et al.</i> (2010); Dyke <i>et al.</i> (2019)
Eastern and northern Greenland	-51 ± 71	21, 22, 23, 25, 26, 27, 28, 29, 30, 667, 669, 670, 671, 791	Håkansson (1973); Tauber & Funder (1975); Olsson (1980)

¹Map number refers to the 'mapno' field in the Calib reservoir age database (<https://calib.org/marine/>).

et al. 2016). The reconstructed ice sheets were calculated on a 5 km resolution grid.

Changes in sea level and topography were calculated using the GIA model SELEN (Spada & Stocchi 2007; de Boer *et al.* 2014). The rheology model used for PaleoMIST is a three layer, spherically concentric Earth (i.e. a 1D) model with an 120 km thick elastic lithosphere, an upper mantle viscosity of 4×10^{20} Pa·s and a lower mantle viscosity of 4×10^{22} Pa·s. In reconstructing the ice sheet, the topography and sea-level changes were iterated several times to account for changes in the ice loading.

Since the Greenland ice sheet contributed only a small amount to sea-level change during the last glacial cycle, it was not a focus of investigation for PaleoMIST 1.0. As a result, the margin history and shear stress values were not scrutinised to the same extent as for the North American and Eurasian ice sheets. The shear stress values were held constant through the entire time period. The margins were drawn through interpolation between the present margin and the inferred LGM margin through interpolation, with minimal considerations of the impacts of ice-sheet dynamics and topography.

The basal shear stress is primarily related to the topographic roughness and basal geology. In Greenland, the basal geology is completely unconstrained, so I divided the regions based only on topography (Gowan *et al.* 2016a). The domain boundaries of equal shear stress are based on the locations of fjords, mountain ranges and relatively flat areas in the interior of Greenland (Fig. 3). The value in each subregion was then tuned to reproduce the ice thickness of the modern ice-sheet configuration. In currently deglaciated coastal shelf regions where the ice sheet interacted with the ocean, the basal shear stress is assumed to be a low value because of the introduction of buoyancy forces and the presence of deforming sediments at the base. The value in each subregion was then tuned to reproduce the ice thickness of the modern ice-sheet configuration. The shear stress values were held to be constant in the reconstruction, though thinning or reduction in elevation of the central parts of the ice sheet during the Holocene (Vinther *et al.* 2009; Lecavalier *et al.* 2013) would imply a reduction in shear stress in the absence of large-scale margin retreat. In general, the shear stress values are relatively high (>100 kPa) around the edges of Greenland, where there is mountainous topography. It is lower (<100 kPa) in the centre where the topography is flatter and the ice sheet – surface elevation gradient becomes limited. This is related to the impact on ice-sheet dynamics of the mountains around the edge of Greenland that impede ice flow from central Greenland (Cuffey & Paterson 2010). The continental shelf areas are set to have a low nominal shear stress (<10 kPa). The low shear stress is expected because of the interactions with the ocean and the fact that the ice

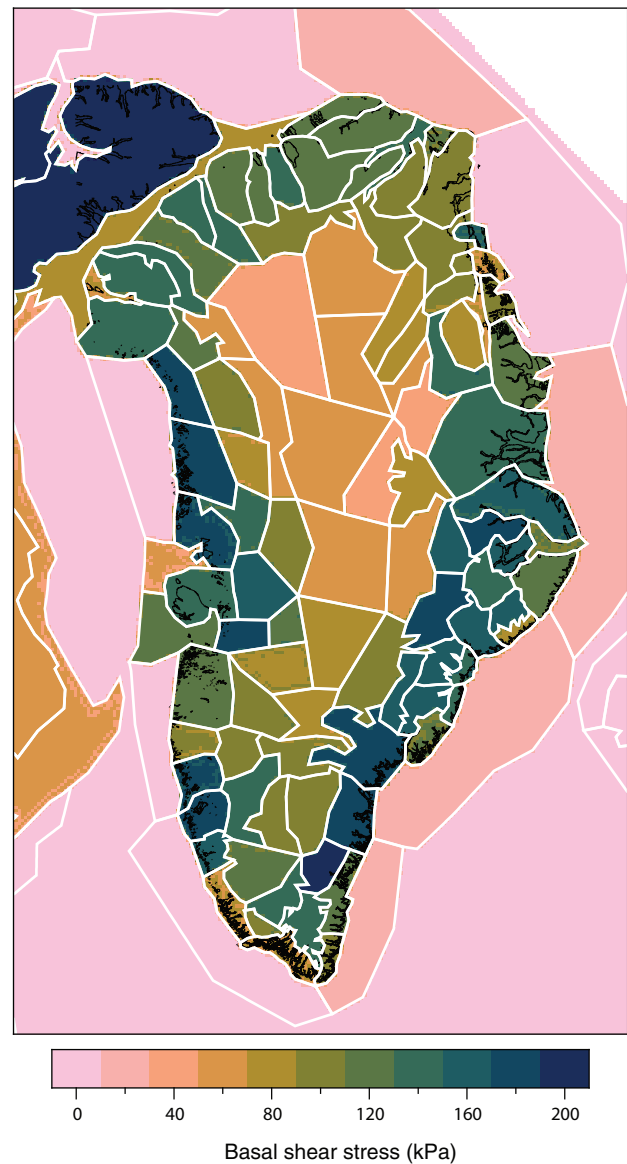


Fig. 3 Basal shear stress values used to reconstruct the Greenland ice sheet.

sheet would be underlain with unconsolidated sediments that would encourage ice flow.

Using the present-day basal shear stress values may cause the ice thickness in the interior of the Greenland ice sheet to be overestimated during the glacial period. The core of the ice sheet may have been thinner than at present because of dynamic effects of softer ice from the glacial period and lower accumulation rates (Reeh 1985; Cuffey & Clow 1997), though it may not be possible to quantify this (Lecavalier *et al.* 2013). In PaleoMIST 1.0, the increase in ice thickness in the centre of the Greenland ice sheet at the LGM varies between 150 and 300 m. If the interior of the ice sheet was thinner than at present during the LGM, it would increase the potential maximum sea-level highstand in coastal regions because of a reduction of forebulge effects.

The margin reconstructions for Greenland during the past 80 000 years was based on a number of inferences

from geological data and previously published reconstructions. The modern margin was extracted from the RTopo-2 data set; Schaffer *et al.* (2016), which defines the grounded part of the Greenland ice sheet. This was also used as the margin at 7.5 kyr BP. For the 5 kyr BP time step, the margin in south-western Greenland was set to retreat about 40 km from the present-day margin, based on evidence of retreat between 10 to 80 km from its current extent in the mid-Holocene (Funder *et al.* 2011b). The 2.5 kyr BP margin was set to be intermediate of the 5 kyr BP and modern margins. The margins from 10 to 17.5 kyr BP were derived from the reconstructions by Dyke (2004). It appears that these margins were drawn using the inaccurate GSHHG coastlines mentioned in Section 2.2, therefore the reconstructed ice sheet will be in error in North Greenland. The LGM extent is based on the reconstruction presented by

Funder *et al.* (2011b), and this is also used as the basis for the margin location to 30 kyr BP. The margin reconstructions for 77.5 to 32.5 yr BP were set to be intermediate of the LGM and present-day margin, with fluctuations to coincide with the timing of Heinrich Events (Andrews & Voelker 2018), and geological constraints reported in a number of studies (Alley *et al.* 2010; Funder *et al.* 2011b; Simon *et al.* 2014; Larsen *et al.* 2018). The Marine Isotope Stage 4 maximum extent was set to 60 kyr BP, with an extent of 25 km landward from the LGM margin. The margin at 80 kyr BP is set to be the same as present.

Figure 4 shows the thickness and volume changes of the Greenland ice sheet since the LGM. The ice volume is reported as sea level equivalent (SLE), which is the ice volume converted to an equivalent amount of ocean-water volume, and divided by the modern area of the ocean

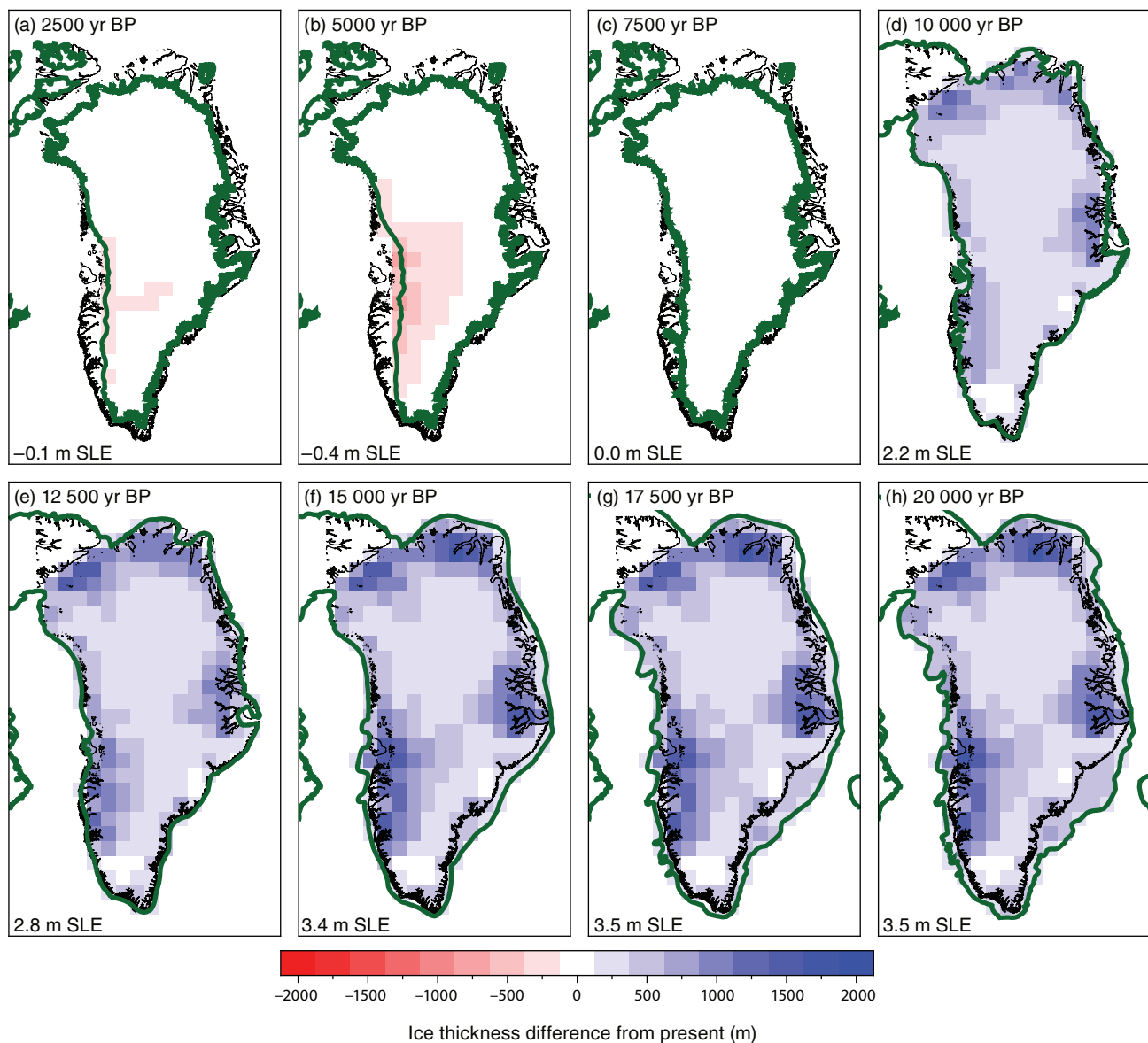


Fig. 4 Difference in ice thickness from the present-day Greenland ice sheet in PaleoMIST 1.0, reported as sea-level equivalents (SLE) at various time slices. The **dark green line** is the location of the (grounded) ice-sheet margin. Time slices are as follows: (a) 2.5 kyr BP. (b) 5 kyr BP. (c) 7.5 kyr BP. (d) 10 kyr BP. (e) 12.5 kyr BP. (f) 15 kyr BP. (g) 17.5 kyr BP. (h) 20 kyr BP.

(361×10^6 km²). The SLE calculation also subtracts the modern ice volume and water volume on the continental shelf. At the LGM, the Greenland ice sheet contributed to about 3.5 m of SLE ice volume to global ice volume, less than 4% of the total excess ice volume in PaleoMIST 1.0. This value is maintained until the time slice at 12.5 kyr BP, when the ice volume is reduced by 0.6 m SLE. At 7.5 kyr BP, the ice margin is set to be the same as present, thus there is essentially no difference in ice volume from the present. The reduced extent margin in western Greenland caused a reduction in ice volume of 0.4 m SLE. Most of the additional ice in the reconstruction at the LGM is located in areas that are currently ice free, with only limited ice thickness gain (<500 m) in much of the interior of the ice sheet.

3.2 Comparison of calculated sea level with proxies and indicators

The calculated sea level and data for selected locations found in Fig. 1 are shown in Fig. 5. Although the

PaleoMIST 1.0 reconstruction has 2500 year time steps, the sea level is calculated by linearly interpolating the ice load to 500 year time steps. This is done to avoid the overestimation of loading caused by the fact that SELEN treats the load as a Heaviside function (i.e. constant ice volume between two time steps). Some of the locations contain data from a broad area where the gradient in the GIA signal is large. Therefore, the calculated sea level after deglaciation within a single location might have a large variations depending on the proximity to the centre of the ice load. This can be seen in the locations with multiple calculated sea-level curves on the figures.

Overall, the calculated sea level from PaleoMIST 1.0 fails to achieve the high relative sea-level values implied by the sea-level proxy and indicator data for the Early Holocene. The only locations that come close are in the vicinity of the Nares Strait, such as Hall Land. The relatively good fit there is likely a consequence of the fact that the neighbouring Inuitian ice sheet was tuned to

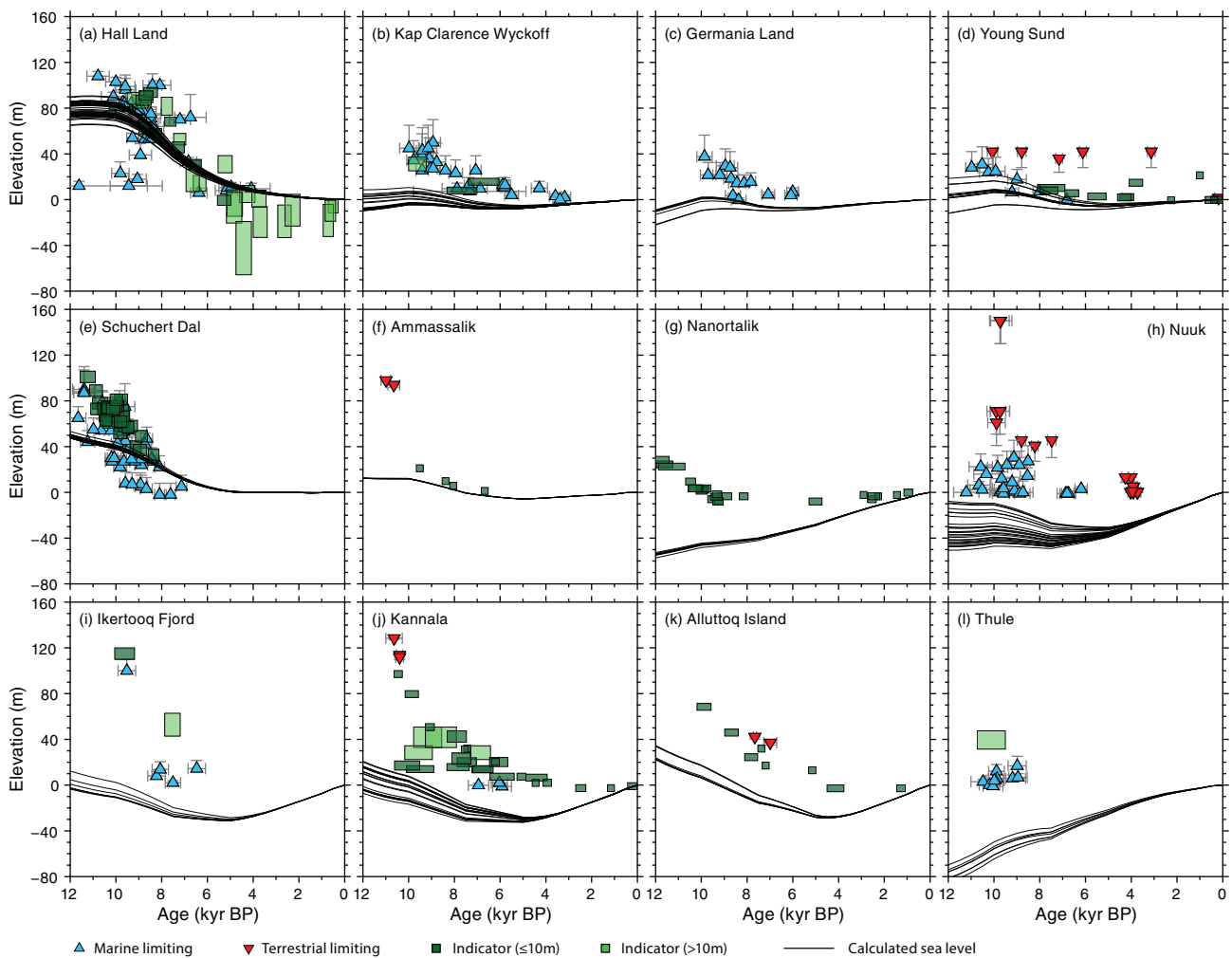


Fig. 5 Plots showing sea-level indicators and proxies for selected subregions around Greenland, and the calculated sea-level curves from PaleoMIST 1.0. A darker shade of green is used for sea-level indicators that have an uncertainty range less than 10 m to emphasise their quality. Since the locations of the data often cover a broad area, there can be a gradient in the sea-level response, and so multiple calculated curves are shown. Locations in Fig. 1 for the following subregions: **(a)** Hall Land **(b)** Kap Clarence Wyckoff **(c)** Germania Land **(d)** Young Sund **(e)** Schuchert Dal **(f)** Ammassalik **(g)** Nanortalik **(h)** Nuuk **(i)** Ikertooq Fjord **(j)** Kannala **(k)** Alluttoq Island **(l)** Thule.

fit sea-level data, although for a different Earth rheology model than that used in PaleoMIST 1.0 (Khosravi 2017). This misfit is particularly pronounced in the southern and western parts of Greenland, such as Nanortalik and Kannala. Many of these sites have tightly constrained sea level histories from isolation basin studies (Long *et al.* 2011), therefore this misfit demonstrates a deficiency in the model.

4 Discussion

4.1 Exploring potential solutions to the mismatch

One of the possible reasons that the calculated sea level was unable to match observations is that the Earth rheology structure used for PaleoMIST may be inappropriate. This would be unsurprising, since the value for lithospheric thickness (120 km) is considered to be appropriate in stable Precambrian cratons, where much of the Laurentide ice sheet was located. Though the core of Greenland is predominantly Precambrian (Henriksen *et al.* 2000), it is also affected by the Cenozoic passage of the Iceland hot spot (Rogozhina *et al.* 2016). Even so, the Earth model used in PaleoMIST is similar to the optimal model for eastern Greenland found by Simpson *et al.* (2009; 120 km lithosphere, 3×10^{20} Pa·s upper mantle and 5×10^{22}) and within the range of optimal models found by (Lecavalier *et al.* 2014). The later study found that there was only limited sensitivity to lower mantle viscosity, a result that is consistent with my own analysis, with the exception of northern Greenland (see Gowan 2023a). Milne *et al.* (2018) found that variations in lithospheric thickness relative to a uniform value of 120 km may be responsible for over 20 m of the observed highstand at the start of the Holocene in some areas. The response to deglaciation may also be influenced by time-variable (transient) viscosity of the upper mantle (Paxman *et al.* 2023).

The other main possibility is that the history of ice-sheet volume is inappropriate. The maximum excess ice volume in PaleoMIST at the LGM is 3.5 m SLE (Fig. 4), which is less than the 4.6 m SLE value estimated by Simpson *et al.* (2009) and 4.7 m SLE estimated by Lecavalier *et al.* (2014). However, it is more than the 3.1 m SLE estimated by Fleming & Lambeck (2004) and the 1.9 m SLE estimated from Tarasov & Peltier (2002). The 2500 time step used for the margin history may also fail to capture the precise timing of the retreat of the ice sheet, which was predicted by Lecavalier *et al.* (2014) to have largely happened between 12 and 10 kyr BP. The PaleoMIST model may initiate ice-sheet retreat too early if this is correct, which would decrease the potential sea-level highstand at 10 kyr BP. The model by Lecavalier

et al. (2014) depicts the western Greenland ice sheet as extending to the shelf edge, in contrast to the more restricted extent that was used in PaleoMIST from Funder *et al.* (2011b). If this is correct, there would be a greater perturbation of the upper mantle response as the excess volume would be spread over a larger area, which would result in a larger highstand.

To address some of these possibilities, I have run a number of additional Earth and ice models, the full results of which can be viewed in the GAPSLIP-PaleoMIST model comparison reports (Gowan 2023a). To highlight some of the possibilities, I have selected two different Earth Models for comparison, one with a lithospheric thickness of 60 km rather than 120 km, and another using the VM5a viscosity model that is used by Peltier *et al.* (2015; Fig. 6). A 60 km thick lithosphere has been inferred from parts of Greenland affected by the Iceland hot spot from the modelling of present-day uplift rates (Khan *et al.* 2016). The model used in Fig. 6 has a slightly different upper and lower mantle viscosity than used by Khan *et al.* (2016), but in the interests of assessing the impact of lithospheric thickness changes, I have not changed them to match. The VM5a model has a 60 km thick lithosphere, a 40 km thick layer below the lithosphere with a viscosity of 1×10^{22} Pa·s, an upper mantle viscosity of 5×10^{20} Pa·s and a lower mantle viscosity (between 660 and 1160 km depth) of 1.6×10^{21} Pa·s. The rest of the lower mantle has a viscosity of 3.2×10^{21} Pa·s. I have also selected an alternative ice-sheet model where the basal shear stress values for Greenland have been increased by 20 kPa prior to 10 kyr BP. This has the effect of increasing the LGM ice volume to 4.8 m SLE, which is closer to the models by Simpson *et al.* (2009) and Lecavalier *et al.* (2014). The four locations shown in Fig. 6 represent the different parts of northern (Kap Clarence Wyckoff), eastern (Schuchert Dal), southern (Nanortalik) and western (Kannala) Greenland.

The results show that at least for northern, eastern and western Greenland, an improved fit can be achieved by reducing the lithospheric thickness, or using the more complex structure of VM5a, without modifications to the ice-volume history. It is possible that the 120 km lithosphere thickness is inappropriate for most of Greenland. The improved fit from the VM5a could be the result of having the thin high-viscosity layer under the lithosphere, which delays the rebound after melting compared to the elastic rheology. The weaker lower mantle may also change the position and increase the rate of collapse of the forebulge of the North American ice sheets. For these regions, increasing the ice thickness only has a relatively small improvement on matching the calculated sea level to the data, at least if the ice-margin history is unchanged. The match in southern Greenland is not substantially improved by either changing the ice thickness or Earth structure, suggesting that substantial

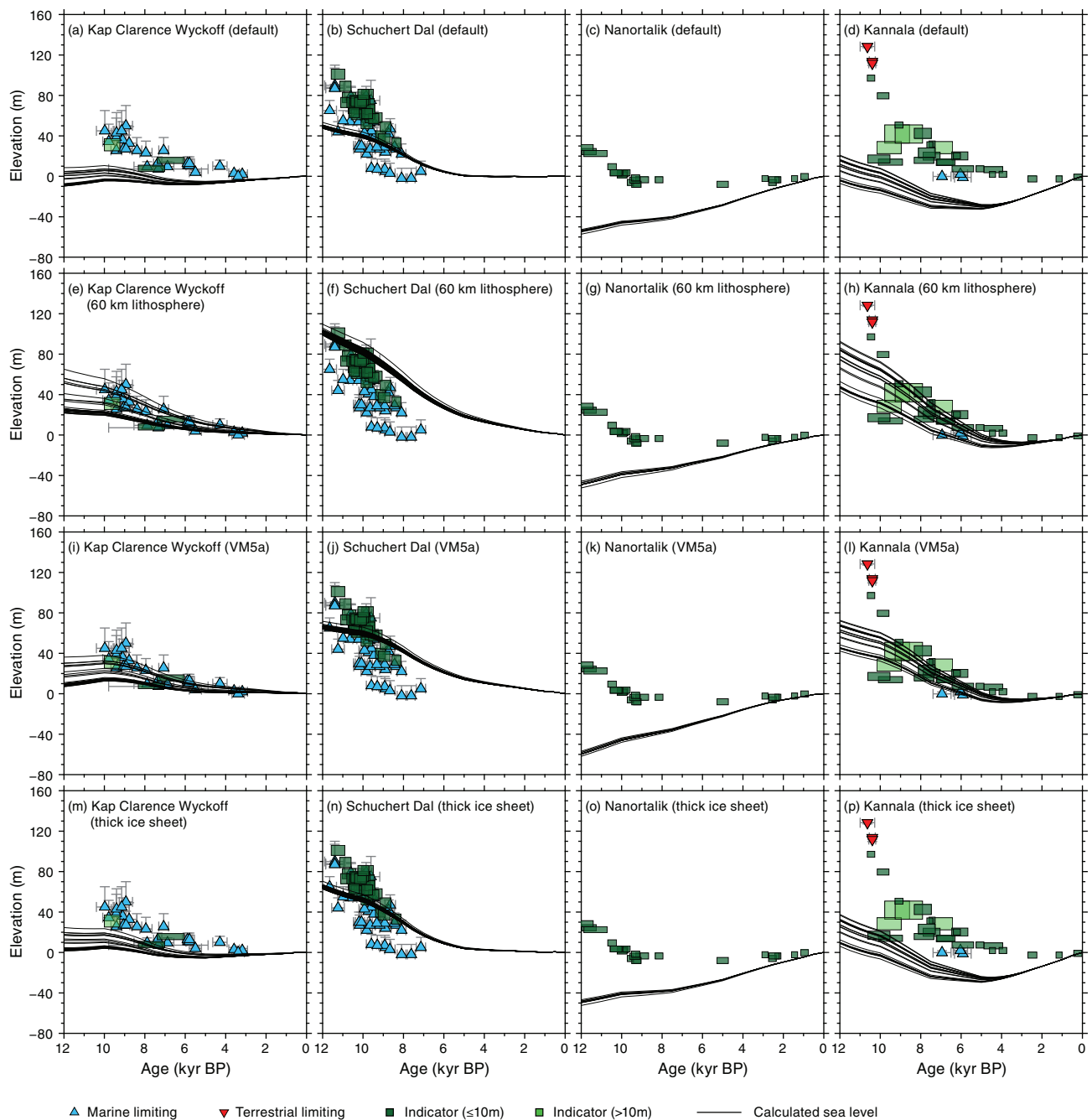


Fig. 6 Plots showing sea-level indicators and proxies for selected subregions around Greenland and the calculated sea-level curves from PaleoMIST 1.0 using (a–d) the default Earth model, (e–h) a 60 km lithosphere thickness rather than 120 km, (i–l) using the VM5a Earth model, and (m–p) using a thicker Greenland ice sheet where the shear stress values before 10 kyr BP have been increased by 20 kPa. Since the locations of the data often cover a broad area within the region, there can be a gradient in the sea-level response, and so there are multiple calculated curves. Locations in Fig. 1. A darker shade of green is used for sea-level indicators that have an uncertainty range less than 10 m to emphasise their quality.

revisions on the basal shear stress and ice-margin history are required to fit these data. This misfit is not surprising since the paleo ice thickness is not substantially different from present in southern Greenland (Fig. 4). In all cases, the fit may be improved by including a more detailed history of margin retreat such as the recently released PaleoGrIS margin reconstruction (Leger *et al.* 2023).

A final possibility is that the resolution of the GIA modelling needs to be increased. The PaleoMIST

reconstruction used in SELEN is composed of disc elements with a radius of approximately 34 km and a spherical harmonic expansion of 256 degrees. These limits were considered appropriate given the preliminary nature of the reconstruction, and the computational expense if the resolution was increased further. If the deep fjords around the margin of Greenland bias the elevation of the elements downwards, the programme may interpret the ice as floating and it will not contribute to loading. This bias could be mitigated

by using higher resolution grid elements or by using a median filter to create the topography rather than an average filter or random sampling. This will be considered in future reconstructions.

4.2 Contributions to global sea level

The contribution to LGM sea level from the Greenland ice sheet in PaleoMIST 1.0 is 3.5 m SLE and represents 3–4% of the LGM ice volume. This value is intermediate of other GIA-based ice-sheet reconstructions (Tarasov & Peltier 2002; Fleming & Lambeck 2004; Simpson *et al.* 2009; Lecavalier *et al.* 2014). In Gowan *et al.* (2022), we concluded that the misfit between the calculated sea level and some far-field sea-level indicators (far from the GIA effects of the ice sheets) was because of the lack of smaller ice caps and glaciers, changes in land-based water storage and thermal expansion in the reconstruction. From the results of this study, it is possible that additional ice volume from Greenland could also contribute to the underestimate of global ice volume at the LGM in PaleoMIST.

The results from this study indicate that there is a certain amount of ambiguity in the Greenland ice sheet's contribution to global sea level at the LGM. The PaleoMIST reconstructed ice sheet, though intermediate of other reconstructions, does not provide a great match to the paleo sea-level observations. More ice, through increased basal shear stress or an extended ice margin, could be added to the reconstruction to reconcile some of these observations, but this can also be countered by accounting for lateral changes in lithosphere thickness and upper mantle viscosity. Some recently collected geological constraints, such as cosmogenic dates from western Greenland (Graham *et al.* 2019; Sbarra *et al.* 2022) and submarine landform features (Ó Cofaigh *et al.* 2013), favour larger ice-sheet configurations.

The consequence of this ambiguity means that it is difficult to constrain the history of the ice sheet for the purposes of predicting the future of the ice sheet. The momentum caused by past changes in ice-sheet dynamics have impacts on the current dynamics of the ice sheet, and may be delaying changes because of current global warming (Yang *et al.* 2022). Whether having a larger (i.e. >4.5 m SLE) or smaller (i.e. <2 m SLE) at the LGM, impacts the current trajectory of ice-sheet retreat should be the subject of further investigation.

4.3 Improvements to the sea-level indicator and proxy database

The sea-level indicator and proxies presented in this study were compiled in a way that is sufficient to evaluate the fit of calculated sea level. However, the database could be improved to reduce the vertical uncertainties

if more details on the survey techniques were found. It may also be possible to determine the elevation with lower uncertainty using modern high-resolution topography data sets. It may be possible to infer the sea-level indicative range for *in situ* marine molluscs that are currently classified as marine limiting through scrutinising the geological context of the deposits, or by using the depth-range inference techniques proposed by Glueder *et al.* (2022). The GAPSLIP database also excludes marine limit-data that may not be possible to directly date using radiocarbon. Marine-limit data are widely available in Greenland (Dyke *et al.* 2005) and it may be possible to assign an age based on regional correlations or via cosmogenic dating techniques. Since the marine limit can be determined through remote sensing, it may be one way to determine the GIA signal in places with few other constraints (e.g. McMartin *et al.* 2022). Finally, since this database relied on the list of references found in Lecavalier *et al.* (2014) for data published prior to 2014, it is possible that key studies containing additional proxies were omitted. I hope to actively update the database, and welcome additional sea-level proxy data for inclusion as they become available.

5. Conclusions

This study has presented a new publicly accessible archive of sea-level indicators and proxies for Greenland as part of the GAPSLIP database. This archive makes it possible to easily assess calculated sea level from GIA models. These data demonstrate that the pre-Holocene PaleoMIST 1.0 ice-sheet reconstruction likely requires additional ice volume in Greenland, particularly in southern Greenland. It is also likely that much of the misfit with sea-level data is attributable to neglecting lateral variations in Earth rheology, and that using a thinner lithosphere will produce a better fit to the data without requiring substantially more ice. Another possibility is that the LGM margin of the ice sheet was more expansive than inferred. The new sea-level data set could be supplemented with additional data and improved with more refined uncertainty estimates.

Acknowledgments

The figures were generated using Generic Mapping Tools (GMT) version 6.4 (Wessel *et al.* 2019). My gratitude goes to the authors of GMT who fixed a couple of issues I was having, and for clarifying some of the aspects of the Greenland coastline reconstruction. Some figures in this manuscript make use of the Scientific Colour Maps (Crameri *et al.* 2020). I also thank Thomas Lorscheid and Alessio Rovere who gave guidance in my port of their tool IMCalc to Python, which is included in GAPSLIP. I also thank Tomohiko Tomita, who has helped me with logistical aspects of my postdoctoral studies, which this paper is part of. I acknowledge PALSEA, a working group of the International Union for Quaternary Sciences (INQUA) and Past Global Changes (PAGES), which in turn received support from the Swiss Academy of Sciences and the Chinese Academy of Sciences. I thank Paolo Stocchi for the

use of his standalone version of SELEN. Lastly, I thank reviewers, William Colgan and Sarah Bradley, for their comments that helped improve the paper.

Additional information

Funding statement

Funding came from an International Postdoctoral Fellowship of Japan Society for the Promotion of Science.

Author contributions

E.J.G compiled the sea level proxy data, performed the analysis and wrote the paper.

Competing interests

There are no competing interests.

Additional files

Plots containing the data-model comparison of all 47 Greenland sites are provided in Supplementary File S1 (<https://doi.org/10.22008/FK2JJQ7NH>). Version 2.0 of the GAPSLIP database is available at Zenodo (Gowan 2023b; <https://doi.org/10.5281/zenodo.8036475>) and is updated on Github: (https://github.com/evangowan/paleo_sea_level). A spreadsheet with all of the paleo sea-level proxies and indicators for Greenland can be found on Zenodo (Gowan 2023c; <https://doi.org/10.5281/zenodo.8036552>). A comparison of all the sites in GAPSLIP with various Earth and ice-sheet models can be found on Zenodo (Gowan 2023a; <https://doi.org/10.5281/zenodo.7923553>).

References

- Alley, R.B. *et al.* 2010: History of the Greenland Ice Sheet: paleoclimatic insights. *Quaternary Science Reviews* **29**, 1728–1756. <https://doi.org/10.1016/j.quascirev.2010.02.007>
- Andrews, J.T. & Voelker, A.H. 2018: 'Heinrich Events' (& sediments): a history of terminology and recommendations for future usage. *Quaternary Science Reviews* **187**, 31–40. <https://doi.org/10.1016/j.quascirev.2018.03.017>
- Baranskaya, A.V., Khan, N.S., Romanenko, F.A., Roy, K., Peltier, W. & Horton, B.P. 2018: A postglacial relative sea-level database for the Russian Arctic coast. *Quaternary Science Reviews* **199**, 188–205. <https://doi.org/10.1016/j.quascirev.2018.07.033>
- Belperio, A.P., Harvey, N. & Bourman, R.P. 2002: Spatial and temporal variability in the Holocene sea-level record of the South Australian coastline. *Sedimentary Geology* **150**, 153–169. [https://doi.org/10.1016/S0037-0738\(01\)00273-1](https://doi.org/10.1016/S0037-0738(01)00273-1)
- Bennike, O. 1995: Palaeoecology of two lake basins from Disko, West Greenland. *Journal of Quaternary Science* **10**, 149–155. <https://doi.org/10.1002/jqs.3390100205>
- Bennike, O. 1997: Quaternary vertebrates from Greenland: a review. *Quaternary Science Reviews* **16**, 899–909. [https://doi.org/10.1016/S0277-3791\(97\)00002-4](https://doi.org/10.1016/S0277-3791(97)00002-4)
- Bennike, O. 2002: Late Quaternary history of Washington Land, North Greenland. *Boreas* **31**, 260–272. <https://doi.org/10.1111/j.1502-3885.2002.tb01072.x>
- Bennike, O. & Kelly, M. 1987: Radiocarbon dating of samples collected during the 1984 expedition to North Greenland. *Rapport Grønlands Geologiske Undersøgelse* **135**, 8–10.
- Bennike, O. & Wagner, B. 2012: Deglaciation chronology, sea-level changes and environmental changes from Holocene lake sediments of Germania Havn Sø, Sabine Ø, northeast Greenland. *Quaternary Research* **78**, 103–109. <https://doi.org/10.1016/j.yqres.2012.03.004>
- Bennike, O. & Weidick, A. 2001: Late Quaternary history around Nioghalvfjærdsfjorden and Jøkelbugten, North-East Greenland. *Boreas* **30**, 205–227. <https://doi.org/10.1111/j.1502-3885.2001.tb01223.x>
- Bennike, O., Björck, S. & Lambeck, K. 2002: Estimates of South Greenland late-glacial ice limits from a new relative sea level curve. *Earth and Planetary Science Letters* **197**, 171–186. [https://doi.org/10.1016/S0012-821X\(02\)00478-8](https://doi.org/10.1016/S0012-821X(02)00478-8)
- Bennike, O., Wagner, B. & Richter, A. 2011: Relative sea level changes during the Holocene in the Sisimiut area, south-western Greenland. *Journal of Quaternary Science* **26**, 353–361. <https://doi.org/10.1002/jqs.1458>
- Berglund, M. 2003: The architecture at three Saqqaq sites in the Nuuk Fjord, Greenland. *Etudes/Inuit/Studies* **27**, 329–346. <https://doi.org/10.7202/010807ar>
- Bierman, P.R., Rood, D.H., Shakun, J.D., Portenga, E.W. & Corbett, L.B. 2018: Directly dating postglacial Greenlandic land-surface emergence at high resolution using in situ ¹⁰Be. *Quaternary Research* **90**, 110–126. <https://doi.org/10.1017/qua.2018.6>
- Björck, S., Bennike, O., Ingólfsson, Ó., Barnekow, L. & Penney, D.N. 1994a: Lake Boksehandsken's earliest postglacial sediments and their palaeoenvironmental implications, Jameson Land, East Greenland. *Boreas* **23**, 459–472. <https://doi.org/10.1111/j.1502-3885.1994.tb00613.x>
- Björck, S., Wohlfarth, B., Bennike, O., Hjort, C. & Persson, T. 1994b: Revision of the early Holocene lake sediment based chronology and event stratigraphy on Hochstetter Forland, NE Greenland. *Boreas* **23**, 513–523. <https://doi.org/10.1111/j.1502-3885.1994.tb00619.x>
- Blake, W. 1987a: Geological survey of Canada radiocarbon dates XXVI. Paper 87–7. Ottawa: Geological Survey of Canada. <https://doi.org/10.4095/122368>
- Blake, W. 1987b: Lake sediments and glacial history in the high arctic; evidence from East-Central Ellesmere Island, Arctic Canada, and from Inglefield Land, Greenland. *Polar Research* **5**, 341–343. <https://doi.org/10.3402/polar.v5i3.6909>
- Blake, W., Jackson, H.R. & Currie, C.G. 1996: Seafloor evidence for glaciation, northernmost Baffin Bay. *Bulletin of the Geological Society of Denmark* **43**, 157–168. <https://doi.org/10.37570/bgsd-1996-43-15>
- Borreggine, M., Latychev, K., Coulson, S., Powell, E.M., Mitrovica, J.X., Milne, G.A. & Alley, R.B. 2023: Sea-level rise in Southwest Greenland as a contributor to viking abandonment. *Proceedings of the National Academy of Sciences* **120**, e2209615120. <https://doi.org/10.1073/pnas.2209615120>
- Briggs, R.D. & Tarasov, L. 2013: How to evaluate model-derived deglaciation chronologies: a case study using Antarctica. *Quaternary Science Reviews* **63**, 109–127. <https://doi.org/10.1016/j.quascirev.2012.11.021>
- Bronk Ramsey, C. 2009: Bayesian analysis of radiocarbon dates. *Radiocarbon* **51**, 337–360. <https://doi.org/10.1017/S0033822200033865>
- Carlson, A.E., Dutton, A., Long, A.J. & Milne, G.A. 2019: PALeo constraints on SEA level rise (PALSEA): ice-sheet and sea-level responses to past climate warming. *Quaternary Science Reviews* **212**, 28–32. <https://doi.org/10.1016/j.quascirev.2019.03.032>
- Christiansen, H.H., Bennike, O., Böcher, J., Elberling, B., Humlum, O. & Jakobsen, B.H. 2002: Holocene environmental reconstruction from deltaic deposits in northeast Greenland. *Journal of Quaternary Science* **17**, 145–160. <https://doi.org/10.1002/jqs.665>
- Coulthard, R.D., Furze, M.F., Pieńkowski, A.J., Nixon, C. & England, J.H. 2010: New marine AR values for Arctic Canada. *Quaternary Geochronology* **5**, 419–434. <https://doi.org/10.1016/j.quageo.2010.03.002>
- Cramer, F., Shephard, G.E. & Heron, P.J. 2020: The misuse of colour in science communication. *Nature Communications* **11**, 5444. <https://doi.org/10.1038/s41467-020-19160-7>
- Cuffey, K.M. & Clow, G.D. 1997: Temperature, accumulation, and ice sheet elevation in central Greenland through the last deglacial transition. *Journal of Geophysical Research: Oceans* **102**, 26383–26396. <https://doi.org/10.1029/96JC03981>
- Cuffey, K.M. & Paterson, W.S.B. 2010: *The physics of glaciers*. Burlington, MA, USA: Elsevier.
- Dalton, A.S., Finkelstein, S.A., Forman, S.L., Barnett, P.J., Pico, T. & Mitrovica, J.X. 2019: Was the Laurentide Ice Sheet significantly reduced during marine isotope stage 3? *Geology* **47**, 111–114. <https://doi.org/10.1130/G45335.1>
- de Boer, B., Stocchi, P. & Van De Wal, R. 2014: A fully coupled 3-D ice-sheet-sea-level model: algorithm and applications. *Geoscientific Model Development* **7**, 2141–2156. <https://doi.org/10.5194/gmd-7-2141-2014>
- de Boer, B., Stocchi, P., Whitehouse, P.L. & van de Wal, R.S. 2017: Current state and future perspectives on coupled ice-sheet – sea-level modelling. *Quaternary Science Reviews* **169**, 13–28. <https://doi.org/10.1016/j.quascirev.2017.05.013>

- Dyke, A.S. 2004: An outline of North American deglaciation with emphasis on central and northern Canada. In: Ehlers, J. *et al.* (eds): Quaternary glaciations-extent and chronology – part II: North America. Cambridge: Elsevier. *Developments in Quaternary Science*, 373–424. [https://doi.org/10.1016/S1571-0866\(04\)80209-4](https://doi.org/10.1016/S1571-0866(04)80209-4)
- Dyke, A.S., Dredge, L.A. & Hodgson, D.A. 2005: North American deglacial marine-and lake-limit surfaces. *Géographie physique et Quaternaire* **59**, 155–185. <https://doi.org/10.7202/014753ar>
- Dyke, A.S., Saville, J.M., Szpak, P., Southon, J.R., Howse, L., Desrosiers, P.M. & Kotar, K. 2019: An assessment of marine reservoir corrections for radiocarbon dates on walrus from the Foxe Basin region of Arctic Canada. *Radiocarbon* **61**, 67–81. <https://doi.org/10.1017/RDC.2018.50>
- Engelhart, S.E. & Horton, B.P. 2012: Holocene sea level database for the Atlantic coast of the United States. *Quaternary Science Reviews* **54**, 12–25. <https://doi.org/10.1016/j.quascirev.2011.09.013>
- England, J. 1985: The late Quaternary history of Hall Land, northwest Greenland. *Canadian Journal of Earth Sciences* **22**, 1394–1408. <https://doi.org/10.1139/e85-147>
- Fleming, K. & Lambeck, K. 2004: Constraints on the Greenland Ice Sheet since the Last Glacial Maximum from sea-level observations and glacial-rebound models. *Quaternary Science Reviews* **23**, 1053–1077. <https://doi.org/10.1016/j.quascirev.2003.11.001>
- Fox-Kemper, B. *et al.* 2021: Ocean, cryosphere and sea level change. In: Masson-Delmotte, V. *et al.* (eds): *Climate change 2021: The physical science basis. Contribution of Working Group I to the Sixth Assessment Report of the Intergovernmental Panel on Climate Change*. 1211–1362. Cambridge and New York: Cambridge University Press. <https://doi.org/10.1017/9781009157896.011>
- Fredh, D. 2008: Holocene relative sea-level changes in the Tasiusaq area, southern Greenland, with focus on the Ta4 basin. Master's thesis, Lund University. <https://lup.lub.lu.se/student-papers/record/2334019> (accessed August 2022).
- Fredskild, B. 1973: Studies in the vegetational history of Greenland. Palaeobotanical investigations of some Holocene lake and bog deposits. Vol. 198. Copenhagen: Museum Tusulanum Press Denmark.
- Fredskild, B. 1983: The Holocene vegetational development of the Godthåbsfjord area, West Greenland. *Meddelelser om Grønland. Geoscience* **10**. Copenhagen: Museum Tusulanum Press.
- Fredskild, B. 1985: The Holocene vegetational development of Tugtulisuaq and Qeqertat, northwest Greenland. *Meddelelser om Grønland Geoscience* **14**, 20.
- Funder, S. 1971: C¹⁴ dates from the Scoresby Sund region, 1971. *Rapport Grønlands Geologiske Undersøgelse* **37**, 57–59. <https://doi.org/10.34194/rapggv.v37.7277>
- Funder, S. 1972: C¹⁴ dates from the Scoresby Sund region, 1972. *Rapport Grønlands Geologiske Undersøgelse* **48**, 115–117. <https://doi.org/10.34194/rapggv.v48.7316>
- Funder, S. 1973: C¹⁴ dates from the Scoresby Sund region, 1973. *Rapport Grønlands Geologiske Undersøgelse* **58**, 75–76. <https://doi.org/10.34194/rapggv.v58.7368>
- Funder, S. 1978: Holocene stratigraphy and vegetation history in the Scoresby Sund area, East Greenland. *Bulletin Grønlands Geologiske Undersøgelse* **129**, 1–66. <https://doi.org/10.34194/bullggv.v129.6671>
- Funder, S. 1982: 14C-dating of samples collected during the 1979 expedition to North Greenland. *Rapport Grønlands Geologiske Undersøgelse* **110**, 9–14. <https://doi.org/10.34194/rapggv.v110.7787>
- Funder, S. 1990a: Descriptive text to Quaternary map of Greenland 1: 500,000, Scoresby Sund. sheet 12. Copenhagen, Denmark: Grønlands Geologiske Undersøgelse.
- Funder, S. 1990b: Late Quaternary stratigraphy and glaciology in the Thule area, Northwest Greenland. *Meddelelser om Grønland, Geoscience* **22**, 63.
- Funder, S. & Abrahamsen, N. 1988: Palynology in a polar desert, eastern North Greenland. *Boreas* **17**, 195–207. <https://doi.org/10.1111/j.1502-3885.1988.tb00546.x>
- Funder, S. & Hansen, L. 1996: The Greenland ice sheet – a model for its culmination and decay during and after the last glacial maximum. *Bulletin of the Geological Society of Denmark* **42**, 137–152. <https://doi.org/10.37570/bgsd-1995-42-12>
- Funder, S *et al.* 2011a: A 10,000-Year record of Arctic Ocean sea-ice variability-view from the beach. *Science* **333**, 747–750. <https://doi.org/10.1126/science.1202760>
- Funder, S., Kjeldsen, K.K., Kjær, K.H. & Ó Cofaigh, C. 2011b: The Greenland Ice Sheet during the past 300,000 years: a review. *Developments in Quaternary Sciences*. **15**, 699–713. <https://doi.org/10.1016/B978-0-444-53447-7.00050-7>
- Foged, N. 1989: The subfossil diatom flora of four geographically widely separated cores in Greenland. *Meddelelser om Grønland* **268**, 75 pp.
- Glueder, A. *et al.* 2022: Calibrated relative sea levels constrain isostatic adjustment and ice history in northwest Greenland. *Quaternary Science Reviews* **293**, 107700. <https://doi.org/10.1016/j.quascirev.2022.107700>
- Gowan, E.J. 2023a: Comparison of the PaleoMIST 1.0 ice sheet margins, ice sheet and paleo-topography reconstruction with paleo sea level indicators, version 2.0. Data set. Zenodo. <https://doi.org/10.5281/zenodo.7923553>
- Gowan, E.J. 2023b: *Evangowan/paleo_sea_level: Gapslip version 2.0.1*. Data set. Zenodo. <https://doi.org/10.5281/zenodo.8036475>
- Gowan, E.J. 2023c: *Paleo sea level proxies and indicators for Greenland*. Data set. Zenodo. <https://doi.org/10.5281/zenodo.8036551>
- Gowan, E.J. *et al.* 2021: A new global ice sheet reconstruction for the past 80000 years. *Nature Communications* **12**, 1199. <https://doi.org/10.1038/s41467-021-21469-w>
- Gowan, E.J., Tregoning, P., Purcell, A., Lea, J., Fransner, O.J., Noormets, R. & Dowdeswell, J.A. 2016a: ICESHEET 1.0: a program to produce paleo-ice sheet reconstructions with minimal assumptions. *Geoscience Model Development* **9**, 1673–1682. <https://doi.org/10.5194/gmd-9-1673-2016>. 2016.
- Gowan, E.J., Tregoning, P., Purcell, A., Montillet, J.P. & McClusky, S. 2016b: A model of the western Laurentide Ice Sheet, using observations of glacial isostatic adjustment. *Quaternary Science Reviews* **139**, 1–16. <https://doi.org/10.1016/j.quascirev.2016.03.003>
- Gowan, E.J. *et al.* 2022: Reply to: towards solving the missing ice problem and the importance of rigorous model data comparisons. *Nature Communications* **13**, 6264. <https://doi.org/10.1038/s41467-022-33954-x>
- Graham, B.L., Briner, J.P., Schweinsberg, A.D., Lifton, N.A. & Bennike, O. 2019: New in situ 14C data indicate the absence of nunataks in west Greenland during the Last Glacial Maximum. *Quaternary Science Reviews* **225**, 105981. <https://doi.org/10.1016/j.quascirev.2019.105981>
- Hall, B.L., Baroni, C. & Denton, G.H. 2008: The most extensive Holocene advance in the Stauning Alper, East Greenland, occurred in the Little Ice Age. *Polar Research* **27**, 128–134. <https://doi.org/10.1111/j.1751-8369.2008.00058.x>
- Hall, B.L., Baroni, C. & Denton, G.H. 2010: Relative sea-level changes, Schuchert Dal, East Greenland, with implications for ice extent in late-glacial and Holocene times. *Quaternary Science Reviews* **29**, 3370–3378. <https://doi.org/10.1016/j.quascirev.2010.03.013>
- Heaton, T.J. *et al.* 2020: Marine20 – The marine radiocarbon age calibration curve (0–55,000 cal BP). *Radiocarbon* **62**, 779–820. <https://doi.org/10.1017/RDC.2020.68>
- Henriksen, N., Higgins, A., Kalsbeek, F. & Pulvertaft, T.C.R. 2000: Greenland from Archaean to Quaternary. Descriptive text to the Geological map of Greenland, 1:2 500 000. *Geology of Greenland Survey Bulletin* **185**, 2–93. <https://doi.org/10.34194/ggub.v185.5197>
- Hinnerson-Berglund, M. 2004: *Mobilitet och estetik. Nuukfjorden på Grønlands västkust som människornas livsvärld för 4000 år sedan*. PhD Thesis. University of Gothenburg. <https://hdl.handle.net/2077/16433> (accessed December 2022).
- Hjort, C. 1973: The vega transgression – a hypsithermal event in Central East Greenland. *Bulletin of the Geological Society of Denmark* **22**, 25–38.
- Hjort, C. 1979: Glaciation in northern East Greenland during the Late Weichselian and Early Flandrian. *Boreas* **8**, 281–296. <https://doi.org/10.1111/j.1502-3885.1979.tb00812.x>
- Hjort, C. 1981: A glacial chronology for northern East Greenland. *Boreas* **10**, 259–274. <https://doi.org/10.1111/j.1502-3885.1981.tb00487.x>
- Hjort, C. 1997: Glaciation, climate history, changing marine levels and the evolution of the Northeast Water polynya. *Journal of Marine Systems* **10**, 23–33. [https://doi.org/10.1016/S0924-7963\(96\)00068-1](https://doi.org/10.1016/S0924-7963(96)00068-1)

- Hjort, C. & Funder, S. 1974: The subfossil occurrence of *Mytilus edulis* L. in central East Greenland. *Boreas* **3**, 23–33. <https://doi.org/10.1111/j.1502-3885.1974.tb00664.x>
- Hogg, A.G. et al.: 2020: SHCal20 Southern Hemisphere calibration, 0–55,000 years cal BP. *Radiocarbon* **62**, 759–778. <https://doi.org/10.1017/RDC.2020.59>
- Hughes, A.L., Gyllencreutz, R., Lohne, Ø.S., Mangerud, J. & Svendsen, J.I. 2016: The last Eurasian ice sheets – a chronological database and time-slice reconstruction, DATED-1. *Boreas* **45**, 1–45. <https://doi.org/10.1111/bor.12142>
- Hughes, T. 1981: Numerical reconstructions of paleo-ice sheets. In: Denton, G.H., Hughes, T.J. (eds): *The last great ice sheets*. 221–261. New York: John Wiley & Sons.
- Hughes, T., Denton, G., Andersen, B., Schilling, D., Fastook, J. & Lingle, C. 1981: The last great ice sheets: a global view. In: Denton, G.H. & Hughes, T.J. (eds): *The last great ice sheets*. 263–317. New York: John Wiley & Sons.
- Håkansson, S. 1972: University of Lund Radiocarbon Dates V. *Radiocarbon* **14**, 380. <https://doi.org/10.1017/S0033822200059440>
- Håkansson, S. 1973: University of Lund Radiocarbon Dates VI. *Radiocarbon* **15**, 493–513. <https://doi.org/10.1017/S0033822200008961>
- Håkansson, S. 1974: University of Lund Radiocarbon Dates VII. *Radiocarbon* **16**, 307–330. <https://doi.org/10.1017/S0033822200059634>
- Håkansson, S. 1975: University of Lund Radiocarbon Dates VIII. *Radiocarbon* **17**, 174–195. <https://doi.org/10.1017/S0033822200002034>
- Håkansson, S. 1976: University of Lund Radiocarbon Dates IX. *Radiocarbon* **18**, 290–320. <https://doi.org/10.1017/S0033822200003179>
- Håkansson, S. 1978: University of Lund Radiocarbon Dates XI. *Radiocarbon* **20**, 416–435. <https://doi.org/10.1017/S0033822200009218>
- Håkansson, S. 1981: University of Lund Radiocarbon Dates XIV. *Radiocarbon* **23**, 384–403. <https://doi.org/10.1017/S0033822200037784>
- Håkansson, S. 1982: University of Lund Radiocarbon Dates XV. *Radiocarbon* **24**, 194–213. <https://doi.org/10.1017/S003382220000504X>
- Håkansson, S. 1987: University of Lund Radiocarbon Dates XX. *Radiocarbon* **29**, 353–379. <https://doi.org/10.1017/S0033822200043769>
- Ingólfsson, Ó., Lyså, A., Funder, S., Möller, P. & Björck, S. 1994: Late Quaternary glacial history of the central west coast of Jameson Land, East Greenland. *Boreas* **23**, 447–458. <https://doi.org/10.1111/j.1502-3885.1994.tb00612.x>
- Ishiwata, T., Okuno, J. & Suganuma, Y. 2021: Excess ice loads in the Indian Ocean sector of East Antarctica during the last glacial period. *Geology* **49**, 1182–1186. <https://doi.org/10.1130/G48830.1>
- Ives, P.C., Levin, B., Robinson, R.D. & Rubin, M. 1964: U. S. Geological Survey Radiocarbon Dates VII. *Radiocarbon* **6**, 37–76. <https://doi.org/10.1017/S0033822200010547>
- Jungner, H. 1979: Radiocarbon dates I. Technical Report. Dating Laboratory, University of Helsinki. Helsinki, Finland. <https://hdl.handle.net/10013/epic.ea2eff4a-ff59-a921-7dda7392d5e1> (accessed November 2022).
- Kelly, M. & Bennike, O. 1985: Quaternary geology of parts of central and western North Greenland: a preliminary account. *Rapport Grønlands Geologiske Undersøgelse* **126**, 111–116. <https://doi.org/10.34194/rapgg.u.v126.7917>
- Kelly, M. & Bennike, O. 1992: Quaternary geology of western and central North Greenland. *Rapport Grønlands Geologiske Undersøgelse* **153**, 1–34. <https://doi.org/10.34194/rapgg.u.v153.8164>
- Kelly, M., Funder, S., Houmark-Nielsen, M., Knudsen, K.L., Kronborg, C., Landvik, J. & Sorby, L. 1999: Quaternary glacial and marine environmental history of northwest Greenland: a review and reappraisal. *Quaternary Science Reviews* **18**, 373–392. [https://doi.org/10.1016/S0277-3791\(98\)00004-3](https://doi.org/10.1016/S0277-3791(98)00004-3)
- Khan, N.S. et al. (HOLSEA working group) 2019: Inception of a global atlas of sea levels since the Last Glacial Maximum. *Quaternary Science Reviews* **220**, 359–371. <https://doi.org/10.1016/j.quascirev.2019.07.016>
- Khan, S.A. et al. 2016: Geodetic measurements reveal similarities between post-Last Glacial Maximum and present-day mass loss from the Greenland ice sheet. *Science Advances* **2**, e1600931. <https://doi.org/10.1126/sciadv.1600931>
- Khosravi, S. 2017: Comparison of the past climate in Northern Canada and Greenland. Master's thesis, University of Bremen. https://www.iup.uni-bremen.de/PEP_master_thesis/thesis_2017/Khosravi_Sara_MScThesis.pdf (accessed June 2022).
- Landvik, J.Y. 1994: The last glaciation of Germania Land and adjacent areas, northeast Greenland. *Journal of Quaternary Science* **9**, 81–92. <https://doi.org/10.1002/jqs.3390090108>
- Landvik, J.Y., Weidick, A. & Hansen, A. 2001: The glacial history of the Hans Tausen Iskappe and the last glaciation of Peary Land, North Greenland. *Meddelelser om Grønland, Geoscience* **39**, 27–44.
- Larcombe, P., Carter, R., Dye, J., Gagan, M. & Johnson, D. 1995: New evidence for episodic post-glacial sea-level rise, central Great Barrier Reef, Australia. *Marine Geology* **127**, 1–44. [https://doi.org/10.1016/0025-3227\(95\)00059-8](https://doi.org/10.1016/0025-3227(95)00059-8)
- Larsen, N.K., Funder, S., Kjær, K.H., Kjeldsen, K.K., Knudsen, M.F. & Linge, H. 2014: Rapid early Holocene ice retreat in West Greenland. *Quaternary Science Reviews* **92**, 310–323. <https://doi.org/10.1016/j.quascirev.2013.05.027>
- Larsen, N.K., Strunk, A., Levy, L.B., Olsen, J., Bjørk, A., Lauridsen, T.L., Jeppesen, E. & Davidson, T.A. 2017: Strong altitudinal control on the response of local glaciers to Holocene climate change in south-west Greenland. *Quaternary Science Reviews* **168**, 69–78. <https://doi.org/10.1016/j.quascirev.2017.05.008>
- Larsen, N.K., Levy, L.B., Carlson, A.E., Buizert, C., Olsen, J., Strunk, A., Bjørk, A.A. & Skov, D.S. 2018: Instability of the Northeast Greenland Ice Stream over the last 45,000 years. *Nature Communications* **9**, 1872. <https://doi.org/10.1038/s41467-018-04312-7>
- Lasca, N.P. 1966: Postglacial dellevelling in Skeldal, Northeast Greenland. *Arctic* **19**, 285–364. <https://doi.org/10.14430/arctic3441>
- Lasher, G.E., Axford, Y., Masterson, A.L., Berman, K. & Larocca, L.J. 2020: Holocene temperature and landscape history of southwest Greenland inferred from isotope and geochemical lake sediment proxies. *Quaternary Science Reviews* **239**, 106358. <https://doi.org/10.1016/j.quascirev.2020.106358>
- Lecavalier, B.S., Milne, G.A., Vinther, B.M., Fisher, D.A., Dyke, A.S. & Simpson, M.J. 2013: Revised estimates of Greenland ice sheet thinning histories based on ice-core records. *Quaternary Science Reviews* **63**, 73–82. <https://doi.org/10.1016/j.quascirev.2012.11.030>
- Lecavalier, B.S. et al. 2014: A model of Greenland ice sheet deglaciation constrained by observations of relative sea level and ice extent. *Quaternary Science Reviews* **102**, 54–84. <https://doi.org/10.1016/j.quascirev.2014.07.018>
- Leger, T.P.M., Clark, C.D., Huynh, C., Jones, S., Ely, J.C., Bradley, S.L., Diemont, C. & Hughes, A.L.C. 2023: A Greenland-wide empirical reconstruction of paleo ice-sheet retreat informed by ice extent markers: Paleogris version 1.0. *Climate of the Past Discussions* **2023**, 1–97. <https://doi.org/10.5194/cp-2023-60>
- Lewis, S.E., Sloss, C.R., Murray-Wallace, C.V., Woodroffe, C.D. & Smithers, S.G. 2013: Post-glacial sea-level changes around the Australian margin: a review. *Quaternary Science Reviews* **74**, 115–138. <https://doi.org/10.1016/j.quascirev.2012.09.006>
- Long, A.J. & Roberts, D.H. 2002: A revised chronology for the 'Fjord Stade' moraine in Disko Bugt, west Greenland. *Journal of Quaternary Science* **17**, 561–579. <https://doi.org/10.1002/jqs.705>
- Long, A.J. & Roberts, D.H. 2003: Late Weichselian deglacial history of Disko Bugt, West Greenland, and the dynamics of the Jakobshavns Isbrae ice stream. *Boreas* **32**, 208–226. <https://doi.org/10.1111/j.1502-3885.2003.tb01438.x>
- Long, A.J., Roberts, D.H. & Rasch, M. 2003: New observations on the relative sea level and deglacial history of Greenland from Innaarsuit, Disko Bugt. *Quaternary Research* **60**, 162–171. [https://doi.org/10.1016/S0033-5894\(03\)00085-1](https://doi.org/10.1016/S0033-5894(03)00085-1)
- Long, A., Roberts, D. & Dawson, S. 2006: Early Holocene history of the west Greenland Ice Sheet and the GH-8.2 event. *Quaternary Science Reviews* **25**, 904–922. <https://doi.org/10.1016/j.quascirev.2005.07.002>
- Long, A.J., Roberts, D.H., Simpson, M.J., Dawson, S., Milne, G.A. & Huybrechts, P. 2008: Late Weichselian relative sea-level changes and ice sheet history in southeast Greenland. *Earth and Planetary Science Letters* **272**, 8–18. <https://doi.org/10.1016/j.epsl.2008.03.042>
- Long, A.J., Roberts, D.H. & Wright, M.R. 1999: Isolation basin stratigraphy and Holocene relative sea-level change on Arveprinsen Ejland, Disko Bugt, West Greenland. *Journal of Quaternary Science* **14**, 323–345. [https://doi.org/10.1002/\(SICI\)1099-1417\(199907\)14:4<323::AID-JQS442>3.0.CO;2-0](https://doi.org/10.1002/(SICI)1099-1417(199907)14:4<323::AID-JQS442>3.0.CO;2-0)

- Long, A.J., Woodroffe, S.A., Dawson, S., Roberts, D.H. & Bryant, C.L. 2009: Late Holocene relative sea level rise and the Neoglacial history of the Greenland ice sheet. *Journal of Quaternary Science* **24**, 345–359. <https://doi.org/10.1002/jqs.1235>
- Long, A.J., Woodroffe, S.A., Roberts, D.H. & Dawson, S. 2011: Isolation basins, sea-level changes and the Holocene history of the Greenland Ice Sheet. *Quaternary Science Reviews* **30**, 3748–3768. <https://doi.org/10.1016/j.quascirev.2011.10.013>
- Lorscheid, T. & Rovere, A. 2019: The indicative meaning calculator-quantification of paleo sea-level relationships by using global wave and tide datasets. *Open Geospatial Data, Software and Standards* **4**, 10. <https://doi.org/10.1186/s40965-019-0069-8>
- Mann, T., Bender, M., Lorscheid, T., Stocchi, P., Vacchi, M., Switzer, A.D. & Rovere, A. 2019: Holocene sea levels in Southeast Asia, Maldives, India and Sri Lanka: The SEAMIS database. *Quaternary Science Reviews* **219**, 112–125. <https://doi.org/10.1016/j.quascirev.2019.07.007>
- McGovern, T.H., Amorosi, T., Perdikaris, S. & Woollett, J. 1996: Vertebrate zooarchaeology of Sandnes V51: Economic change at a chieftain's farm in West Greenland. *Arctic Anthropology* **33**, 94–121. <https://www.jstor.org/stable/40316414> (accessed 31 August 2022).
- McMartin, I., Gauthier, M.S. & Page, A.V. 2022: Updated post-glacial marine limits along western Hudson Bay, central mainland Nunavut and northern Manitoba. Technical Report. Ottawa: Natural Resources Canada. <https://doi.org/10.4095/330940>
- McNeely, R. & Brennan, J. 2005: Geological Survey of Canada revised shell dates. Open File 5019. Ottawa: Geological Survey of Canada. <https://doi.org/10.4095/221215>
- McNeely, R. & McCuaig, S. 1991: Geological Survey of Canada radiocarbon dates XXIX. Paper 89-7. Ottawa: Geological Survey of Canada. <https://doi.org/10.4095/132453>
- McNeely, R., Dyke, A. & Southon, J. 2006: Canadian marine reservoir ages, preliminary data assessment. Open File 5049. Ottawa: Geological Survey of Canada. <https://doi.org/10.4095/221564>
- Milne, G.A., Latychev, K., Schaeffer, A., Crowley, J.W., Lecavalier, B.S. & Audette, A. 2018: The influence of lateral Earth structure on glacial isostatic adjustment in Greenland. *Geophysical Journal International* **214**, 1252–1266. <https://doi.org/10.1093/gji/ggy189>
- Morlighem, M. *et al.* 2017: BedMachine v3: complete bed topography and ocean bathymetry mapping of Greenland from multibeam echo sounding combined with mass conservation. *Geophysical Research Letters* **44**, 11 051–11 061. <https://doi.org/10.1002/2017GL074954>
- Morlighem, M. *et al.* 2022: Icebridge bedmachine Greenland, version 5. Data set. Boulder: NASA National Snow and Ice Data Center Distributed Active Archive Center. <https://doi.org/10.5067/GMEVBWFLWA7X>
- Möller, P., Larsen, N.K., Kjær, K.H., Funder, S., Schomacker, A., Linge, H. & Fabel, D. 2010: Early to middle Holocene valley glaciations on northernmost Greenland. *Quaternary Science Reviews* **29**, 3379–3398. <https://doi.org/10.1016/j.quascirev.2010.06.044>
- Mörner, N.A. & Funder, S. 1990: C-14 dating of samples collected during the NORDQUA 86 expedition, and notes on the marine reservoir effect. In: Funder, S. (ed.): Late quaternary stratigraphy and glaciology in the Thule area, Northwest Greenland. Commission for Scientific Investigations in Greenland. Meddelelser om Grønland Geoscience **22**, 57–59.
- Olsson, I.U. 1980: Content of 14C in marine mammals from Northern Europe. *Radiocarbon* **22**, 662–675. <https://doi.org/10.1017/S0033822200010031>
- Ó Cofaigh, C. *et al.* 2013: An extensive and dynamic ice sheet on the West Greenland shelf during the last glacial cycle. *Geology* **41**, 219–222. <https://doi.org/10.1130/G33759.1>
- Paxman, G.J.G., Lau, H.C.P., Austermann, J., Holtzman, B.K. & Havlin, C. 2023: Inference of the timescale-dependent apparent viscosity structure in the upper mantle beneath Greenland. *AGU Advances* **4**, e2022AV000751. <https://doi.org/10.1029/2022AV000751>
- Pedersen, J.B.T., Kroon, A. & Jakobsen, B.H. 2011: Holocene sea-level reconstruction in the Young Sound region, Northeast Greenland. *Journal of Quaternary Science* **26**, 219–226. <https://doi.org/10.1002/jqs.1449>
- Peltier, W. 2004: Global glacial isostasy and the surface of the ice-age Earth: the ICE-5G (VM2) model and GRACE. *Annual Review of Earth and Planetary Sciences* **32**, 111–149. <https://doi.org/10.1146/annurev.earth.32.082503.144359>
- Peltier, W.R., Argus, D.F. & Drummond, R. 2015: Space geodesy constrains ice age terminal deglaciation: The global ICE-6G_C (VM5a) model. *Journal of Geophysical Research: Solid Earth* **120**, 450–487. <https://doi.org/10.1002/2014JB011176>
- RAISED Consortium *et al.* 2014: A community-based geological reconstruction of Antarctic Ice Sheet deglaciation since the Last Glacial Maximum. *Quaternary Science Reviews* **100**, 1–9. <https://doi.org/10.1016/j.quascirev.2014.06.025>
- Randsalu, L. 2008: Holocene relative sea-level changes in the Tasiusaq area, southern Greenland, with focus on the Ta1 and Ta3 basins. Master's thesis. Lund University. <https://lup.lub.lu.se/studentt-papers/record/1320376> (accessed August 2022).
- Rasch, M. 1997: A compilation of radiocarbon dates from Disko Bugt, Central West Greenland. *Geografisk Tidsskrift – Danish Journal of Geography* **97**, 143–159. <https://doi.org/10.1080/00167223.1997.10649400>
- Reeh, N. 1985: Was the Greenland ice sheet thinner in the late Wisconsinan than now? *Nature* **317**, 797–799. <https://doi.org/10.1038/317797a0>
- Reimer, P.J. & Reimer, R.W. 2001: A marine reservoir correction database and on-line interface. *Radiocarbon* **43**, 461–463. <https://doi.org/10.1017/S0033822200038339>
- Reimer, P.J. *et al.* 2020: The IntCal20 Northern Hemisphere radiocarbon age calibration curve (0–55 cal kBP). *Radiocarbon* **62**, 725–757. <https://doi.org/10.1017/RDC.2020.41>
- Rogozhina, I. *et al.* 2016: Melting at the base of the Greenland ice sheet explained by Iceland hotspot history. *Nature Geoscience* **9**, 366–369. <https://doi.org/10.1038/ngeo2689>
- Rosentau, A. *et al.* 2021: A Holocene relative sea-level database for the Baltic Sea. *Quaternary Science Reviews* **266**, 107071. <https://doi.org/10.1016/j.quascirev.2021.107071>
- Rovere, A. *et al.* 2016: The analysis of Last Interglacial (MIS 5e) relative sea-level indicators: reconstructing sea-level in a warmer world. *Earth-Science Reviews* **159**, 404–427. <https://doi.org/10.1016/j.earscirev.2016.06.006>
- Rubin, M. & Alexander, C. 1960: U. S. Geological survey radiocarbon dates V. *Radiocarbon* **2**, 129–185. <https://doi.org/10.1017/S1061592X00020652>
- Sbarra, C.M., Briner, J.P., Graham, B.L., Poinar, K., Thomas, E.K. & Young, N.E. 2022: Evidence for a more extensive Greenland Ice Sheet in southwestern Greenland during the Last Glacial Maximum. *Geosphere* **18**, 1316–1329. <https://doi.org/10.1130/GES02432.1>
- Schaffer, J., Timmermann, R., Arndt, J.E., Kristensen, S.S., Mayer, C., Morlighem, M. & Steinhage, D. 2016: A global, high-resolution data set of ice sheet topography, cavity geometry, and ocean bathymetry. *Earth System Science Data* **8**, 543–557. <https://doi.org/10.5194/essd-8-543-2016>
- Simon, Q., Hillaire-Marcel, C., St-Onge, G. & Andrews, J.T. 2014: North-eastern Laurentide, western Greenland and southern Inuitian ice stream dynamics during the last glacial cycle. *Journal of Quaternary Science* **29**, 14–26. <https://doi.org/10.1002/jqs.2648>
- Simpson, M.J.R., Milne, G.A., Huybrechts, P. & Long, A.J. 2009: Calibrating a glaciological model of the Greenland ice sheet from the Last Glacial Maximum to present-day using field observations of relative sea level and ice extent. *Quaternary Science Reviews* **28**, 1631–1657. <https://doi.org/10.1016/j.quascirev.2009.03.004>
- Sloss, C.R. & Murray-Wallace, C.V., Jones, B.G. 2007: Holocene sea-level change on the southeast coast of Australia: a review. *The Holocene* **17**, 999–1014. <https://doi.org/10.1177/0959683607082415>
- Souza, P.E., Sohbati, R., Murray, A.S., Clemmensen, L.B., Kroon, A. & Nielsen, L. 2021: Optical dating of cobble surfaces determines the chronology of Holocene beach ridges in Greenland. *Boreas* **50**, 606–618. <https://doi.org/10.1111/bor.12507>
- Spada, G. & Stocchi, P. 2007: SELEN: a Fortran 90 program for solving the 'sea-level equation'. *Computers & Geosciences* **33**, 538–562. <https://doi.org/10.1016/j.cageo.2006.08.006>
- Sparrenbom, C.J., Bennike, O., Björck, S. & Lambeck, K. 2006a: Holocene relative sea-level changes in the Qaqortoq area, southern Greenland. *Boreas* **35**, 171–187. <https://doi.org/10.1111/j.1502-3885.2006.tb01148.x>
- Sparrenbom, C.J., Bennike, O., Björck, S. & Lambeck, K. 2006b: Relative sea-level changes since 15 000 cal. yr BP in the Nanortalik area, southern Greenland. *Journal of Quaternary Science* **21**, 29–48. <https://doi.org/10.1002/jqs.940>

- Steffen, R., Steffen, H., Weiss, R., Lecavalier, B.S., Milne, G.A., Woodroffe, S.A. & Bennike, O. 2020: Early Holocene Greenland-ice mass loss likely triggered earthquakes and tsunamis. *Earth and Planetary Science Letters* **546**, 116443. <https://doi.org/10.1016/j.epsl.2020.116443>
- Storms, J.E.A., de Winter, I.L., Overeem, I., Drijkoningen, G.G. & Lykke-Andersen, H. 2012: The Holocene sedimentary history of the Kangerlussuaq Fjord-valley fill, West Greenland. *Quaternary Science Reviews* **35**, 29–50. <https://doi.org/10.1016/j.quascirev.2011.12.014>
- Street, F.A. 1977: Deglaciation and Marine Paleoclimates, Schuchert Dal, Scoresby Sund, East Greenland. *Arctic and Alpine Research* **9**, 421–426. <https://doi.org/10.1080/00040851.1977.12003935>
- Strunk, A., Larsen, N.K., Nilsson, A., Seidenkrantz, M.S., Levy, L.B., Olsen, J. & Lauridsen, T.L. 2018: Relative sea-level changes and ice sheet history in Finderup Land, North Greenland. *Frontiers in Earth Science* **6**, 1–15. <https://doi.org/10.3389/feart.2018.00129>
- Stuiver, M. & Polach, H.A. 1977: Discussion reporting of ¹⁴C data. *Radiocarbon* **19**, 355–363. <https://doi.org/10.1017/S0033822200003672>
- Tarasov, L. & Peltier, W.R. 2002: Greenland glacial history and local geodynamic consequences. *Geophysical Journal International* **150**, 198–229. <https://doi.org/10.1046/j.1365-246X.2002.01702.x>
- Tauber, H. 1960: Copenhagen radiocarbon dates IV. *Radiocarbon* **2**, 12–25. <https://doi.org/10.1017/S1061592X00020561>
- Tauber, H. 1961: Danske kulstof-14 dateringsresultater I (Danish carbon-14 dating results I). *Meddelelser fra Dansk Geologisk Forening* **14**, 386–405. <https://2dgf.dk/xpdf/bull-1961-14-4-386-405.pdf> (accessed February 2023).
- Tauber, H. 1964: Copenhagen radiocarbon dates VI. *Radiocarbon* **6**, 215–225. <https://doi.org/10.1017/S0033822200010699>
- Tauber, H. 1966: Copenhagen radiocarbon dates VII. *Radiocarbon* **8**, 213–234. <https://doi.org/10.1017/S0033822200000126>
- Tauber, H. & Funder, S. 1975: C14 content of recent molluscs from Scoresby Sund, central East Greenland. *Rapport Grønlands Geologiske Undersøgelse* **75**, 95–99. <https://doi.org/10.34194/rapggv.v75.7460>
- Ten Brink, N.W. 1975: Holocene history of the Greenland ice sheet based on radiocarbon-dated moraines in West Greenland. *Bulletin Grønlands Geologiske Undersøgelse* **113**, 1–44. <https://doi.org/10.34194/bullggv.v113.6654>
- Ten Brink, N.W. & Weidick, A. 1974: Greenland ice sheet history since the last glaciation. *Quaternary Research* **4**, 429–440. [https://doi.org/10.1016/0033-5894\(74\)90038-6](https://doi.org/10.1016/0033-5894(74)90038-6)
- Trautman, M.A. 1963: Isotopes, Inc. Radiocarbon measurements III. *Radiocarbon* **5**, 62–79. <https://doi.org/10.1017/S0033822200036791>
- Vacchi, M., Engelhart, S.E., Nikitina, D., Ashe, E.L., Peltier, W.R., Roy, K., Kopp, R.E. & Horton, B.P. 2018: Postglacial relative sea-level histories along the eastern Canadian coastline. *Quaternary Science Reviews* **201**, 124–146. <https://doi.org/10.1016/j.quascirev.2018.09.043>
- van Tatenhove, F.G.M., van der Meer, J.J.M. & Koster, E.A. 1996: Implications for deglaciation chronology from new AMS age determinations in Central West Greenland. *Quaternary Research* **45**, 245–253. <https://doi.org/10.1006/qres.1996.0025>
- Vink, A., Steffen, H., Reinhardt, L. & Kaufmann, G. 2007: Holocene relative sea-level change, isostatic subsidence and the radial viscosity structure of the mantle of northwest Europe (Belgium, the Netherlands, Germany, southern North Sea). *Quaternary Science Reviews* **26**, 3249–3275. <https://doi.org/10.1016/j.quascirev.2007.07.014>
- Vinther, B.M. *et al.* 2009: Holocene thinning of the Greenland ice sheet. *Nature* **461**, 385–388. <https://doi.org/10.1038/nature08355>
- Washburn, A.L. & Stuiver, M. 1962: Radiocarbon-dated postglacial delevelling in Northeast Greenland and its implications. *Arctic* **15**, 66–73. <https://doi.org/10.14430/arctic3558>
- Weidick, A. 1968: Observations on some Holocene glacier fluctuations in West Greenland. *Bulletin Grønlands Geologiske Undersøgelse* **73**, 1–202. <https://doi.org/10.34194/bullggv.v73.6611>
- Weidick, A. 1972a: C14 dating of survey material performed in 1971. *Rapport Grønlands Geologiske Undersøgelse* **45**, 58–67. <https://doi.org/10.34194/rapggv.v45.7303>
- Weidick, A. 1972b: Holocene shore-lines and glacial stages in Greenland – an attempt at correlation. *Rapport Grønlands Geologiske Undersøgelse* **41**, 1–39. <https://doi.org/10.34194/rapggv.v41.7281>
- Weidick, A. 1973: C14 dating of survey material performed in 1972. *Rapport Grønlands Geologiske Undersøgelse* **55**, 66–75. <https://doi.org/10.34194/rapggv.v55.7356>
- Weidick, A. 1974: C14 dating of survey material performed in 1973. *Rapport Grønlands Geologiske Undersøgelse* **66**, 42–45. <https://doi.org/10.34194/rapggv.v66.7402>
- Weidick, A. 1975: C14 dating of survey material performed in 1974. *Rapport Grønlands Geologiske Undersøgelse* **75**, 19–20. <https://doi.org/10.34194/rapggv.v75.7436>
- Weidick, A. 1976: C14 dating of survey material carried out in 1975. *Rapport Grønlands Geologiske Undersøgelse* **80**, 136–144. <https://doi.org/10.34194/rapggv.v80.7507>
- Weidick, A. 1977: C14 dating of survey material carried out in 1976. *Rapport Grønlands Geologiske Undersøgelse* **85**, 127–129. <https://doi.org/10.34194/rapggv.v85.7545>
- Weidick, A., Bennike, O., Citterio, M. & Nørgaard-Pedersen, N. 2012: Neoglacial and historical glacier changes around Kangarsuneq fjord in southern West Greenland. *Geological Survey of Denmark and Greenland Bulletin* **27**, 1–68. <https://doi.org/10.34194/geusb.v27.4694>
- Wessel, P. & Smith, W.H.F. 1996: A global, self-consistent, hierarchical, high-resolution shoreline database. *Journal of Geophysical Research: Solid Earth* **101**, 8741–8743. <https://doi.org/10.1029/96JB00104>
- Wessel, P., Luis, J.F., Uieda, L., Scharroo, R., Wobbe, F., Smith, W.H.F. & Tian, D. 2019: The generic mapping tools Version 6. *Geochemistry, Geophysics, Geosystems* **20**, 5556–5564. <https://doi.org/10.1029/2019GC008515>
- Woodroffe, S.A., Long, A.J., Lecavalier, B.S., Milne, G.A. & Bryant, C.L. 2014: Using relative sea-level data to constrain the deglacial and Holocene history of southern Greenland. *Quaternary Science Reviews* **92**, 345–356. <https://doi.org/10.1016/j.quascirev.2013.09.008>
- Yang, H. *et al.* 2022: Impact of paleoclimate on present and future evolution of the Greenland Ice Sheet. *PLoS One* **17**, e0259816. <https://doi.org/10.1371/journal.pone.0259816>